JGR Oceans

RESEARCH ARTICLE
10.1029/2024JC021061

Special Collection:
The Arctic Ocean's changing Beaufort Gyre

Can the Marked Arctic Ocean Freshwater Content Increases of the Last Two Decades Be Explained Within Observational Uncertainty?

Isabela Alexander-Astiz Le Bras[1] and **Mary-Louise Timmermans**[2]

[1]Department of Physical Oceanography, Woods Hole Oceanographic Institution, Woods Hole, MA, USA, [2]Department of Earth and Planetary Sciences, Yale University, New Haven, CT, USA

Abstract The freshwater content of the Arctic Ocean has increased dramatically in the last two decades, particularly in the Beaufort Gyre. However, quantifying the sources of this change is an observational challenge and has historically been limited by methodological differences across studies. Here we derive observation-based freshwater budgets from volume and mass budgets for the Arctic Ocean and the Beaufort Gyre from 2003 to 2020. Our budgets include all sources and sinks (river runoff, precipitation minus evaporation, land ice melt, sea ice export, sea ice melt, and ocean fluxes) as well as volume and mass storage terms measured by satellite. We find that Arctic freshwater changes are dominated by changes in the Beaufort Gyre, and we reconcile this with previous studies that argue for freshwater compensation between the Beaufort Gyre and the rest of the Arctic. We use inverse methods to close the volume and mass budgets within observational uncertainty and link the observed Arctic freshwater changes to the sources and sinks. Our budget analysis demonstrates that small changes to the ocean fluxes (smaller than we can measure) can account for all freshwater storage changes in the Arctic, highlighting the need for more careful accounting and detailed ocean observations in this rapidly changing environment.

Plain Language Summary Vast amounts of freshwater flow into the Arctic Ocean from rivers, rain, snow, and ice melt. It is important to better understand and account for these freshwater flows because they are changing under global warming and themselves influencing global ocean circulation and climate. However it remains challenging to take scientific measurements in the Arctic Ocean and its margins. In this study we add up the volume and mass of all the water that flows into and out of the Arctic Ocean and relate this sum to changes in Arctic Ocean volume and mass measured by satellites. Because the Arctic Ocean's density is set by salinity (fresher water sits atop saltier water), and density is the ratio of mass and volume, we can connect our volume and mass budgets to changes in Arctic Ocean salinity. We find that ocean fluxes likely control Arctic Ocean salinity and suggest that these ocean fluxes should be the focus of future studies and measurements.

Key Points:

- We build observation-based Arctic Ocean and Beaufort Gyre mass, volume, and freshwater budgets and close them using inverse methods
- We find little freshwater compensation between the Beaufort Gyre and the rest of the Arctic Ocean, in contrast with previous studies
- Ocean fluxes can account for all interannual Arctic Ocean freshwater content changes from 2003 to 2020

Supporting Information:

Supporting Information may be found in the online version of this article.

Correspondence to:

I. A.-A. Le Bras,
ilebras@whoi.edu

Citation:

Le Bras, I. A.-A., & Timmermans, M.-L. (2025). Can the marked Arctic Ocean freshwater content increases of the last two decades be explained within observational uncertainty? *Journal of Geophysical Research: Oceans*, *130*, e2024JC021061. https://doi.org/10.1029/2024JC021061

Received 23 FEB 2024
Accepted 27 JAN 2025

Author Contributions:

Conceptualization: Isabela Alexander-Astiz Le Bras
Formal analysis: Isabela Alexander-Astiz Le Bras
Funding acquisition: Isabela Alexander-Astiz Le Bras, Mary-Louise Timmermans
Investigation: Isabela Alexander-Astiz Le Bras
Methodology: Isabela Alexander-Astiz Le Bras, Mary-Louise Timmermans
Visualization: Isabela Alexander-Astiz Le Bras
Writing – original draft: Isabela Alexander-Astiz Le Bras
Writing – review & editing: Mary-Louise Timmermans

1. Introduction

Our general understanding of the Arctic Ocean's freshwater budget has not changed significantly since it was characterized by Aagaard and Carmack (1989). Relatively fresh Pacific Waters and warm, salty Atlantic Waters flow into the Arctic and low salinity waters flow out of the Arctic into the Atlantic along the margins of Greenland as well as through the Canadian Arctic Archipelago (Carmack, 2007). The primary source of zero salinity freshwater to the Arctic Ocean is river runoff, followed by precipitation minus evaporation (Haine et al., 2015); sea ice has a significant seasonal cycle of growth and melt, but is exported from the Arctic in the net (Ricker et al., 2018); and glacial melt is still a relatively small source of freshwater to the Arctic Ocean (Bamber et al., 2018a, 2018b). However, a detailed quantification of the Arctic Ocean's freshwater budget remains elusive as observations are particularly sparse in this harsh and remote region.

The last few decades have also been a period of marked Arctic change: sea ice has been in decline (Meier & Stroeve, 2022) and the Beaufort Gyre has accumulated a volume of freshwater at least as large as the Great Salinity Anomaly of the 1970s (Proshutinsky et al., 2019). If released from the Beaufort Gyre, this freshwater could affect ocean circulation, sea ice conditions, and ecosystems (Carmack et al., 2016). In particular, a freshwater release to the subpolar North Atlantic would likely disrupt deep water formation in the Labrador Sea, air-sea fluxes, and potentially the Atlantic Meridional Overturning Circulation (Haine et al., 2023; Zhang

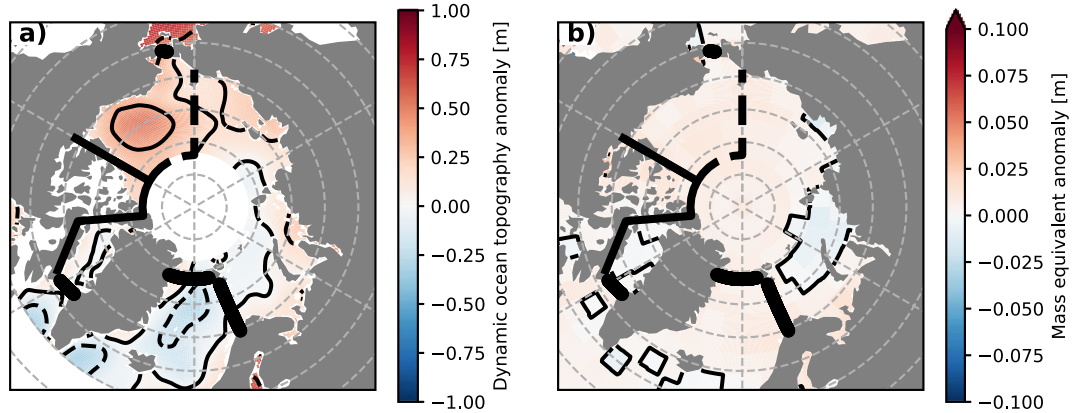

Figure 1. Time mean satellite fields from 2003 to 2014, when there was the best satellite coverage. (a) Mean dynamic ocean topography anomaly. (b) Mean mass equivalent anomaly from Gravity Recovery and Climate Experiment. Both panels show the locations of the Arctic Straits in thick lines, with the thinner black line showing the boundary used around the Canadian Arctic Archipelago. The Full Arctic region north of the Straits includes Baffin Bay, but not the Canadian Arctic Archipelago. Dashed lines indicate the Beaufort Gyre region. The white area in panel (a) north of 81.5°N is the "pole hole," where altimeter data are not available pre-2011.

et al., 2021). These observed changes and their associated local and global climate influences add urgency to better understanding the Arctic Ocean's changing freshwater budget.

In a relatively recent, comprehensive review, Haine et al. (2015) cannot account for the overall Arctic Ocean freshwater changes with changes in the sources; they report that the freshwater content has increased more than the sources have changed, but the uncertainty remains significant. Synthesis efforts such as Haine et al.'s (2015) (see also Carmack et al., 2016; Serreze et al., 2006; Solomon et al., 2021) are limited by the fact that there is widespread use of reference salinities in the literature, which oceanic freshwater transports can be sensitive to, but pure freshwater sources are not (Schauer & Losch, 2019).

Oceanic freshwater fluxes into the Arctic have been quantified extensively by Tsubouchi et al. (2012); Tsubouchi et al. (2018, 2023), who merged all available ocean observations in a self-consistent inverse model. They use the boundary-averaged salinity as a reference salinity so that their freshwater fluxes are more physically meaningful and ensure that mass, salinity, and heat are conserved in their analysis (Bacon et al., 2015). However, Tsubouchi et al. do not include time-varying observations of freshwater sources and sinks or explicitly account for freshwater storage, which Bacon et al. (2022) highlight as an important next step. In other words, it remains unclear how the oceanic freshwater fluxes into the Arctic Ocean are linked to changes in freshwater content.

In this study, we build a consistent time-varying Arctic Ocean freshwater budget based on observations from 2003 to 2020, as well as a budget for the Beaufort Gyre (Figure 1). We note that there are some key differences between the freshwater budgets we present here and those typically presented in the oceanographic literature (e.g., Haine et al., 2015; Proshutinsky et al., 2019). First, we circumvent the issue of reference salinities by building volume and mass budgets and differencing them to retrieve the steric budget, which is approximately equivalent to the freshwater budget in the Arctic. Our budgets are for the full water column, they are not bounded by a reference salinity from below (but this does not influence the interpretation of our budgets significantly). Second, we analyze net oceanic volume and mass fluxes into each control volume rather than considering the contribution from individual Straits or water masses. This was done because Tsubouchi et al. (2023) present detailed analyses of ocean freshwater fluxes into the Arctic and because our intention is to focus on the overall balances in this first presentation of our approach.

Giles et al. (2012) used satellite measurements to link steric changes with freshwater content changes in the Beaufort Gyre (McPhee et al., 2009; Proshutinsky et al., 2009), capitalizing on the fact that Arctic Ocean density is dominated by salinity. This relationship was also used by Morison et al. (2012), who suggested that the increase in freshwater content in the Beaufort Gyre was at least partially compensated for by decreases in other parts of the Arctic, and more recently by Lin et al. (2023), who report that Beaufort Gyre freshwater content has plateaued since the rapid increase in the 2000s. However the degree to which freshwater increases in the Beaufort Gyre are

compensated by decreases in other parts of the Arctic remains unclear (see also McPhee et al., 2009; Solomon et al., 2021). We place these changes in the Beaufort Gyre steric height in the context of changes in the full Arctic and link them directly to observation-based estimates of sources and sinks (river runoff, precipitation minus evaporation, land ice melt, sea ice export, sea ice melt, and ocean fluxes). In addition to examining the long term changes, we analyze the seasonal variability in our budgets and link these to previous work.

We first outline our budget framework (Section 2.1) and link Arctic Ocean steric budgets to freshwater budgets (Section 2.2). Then we introduce the data sources for each budget term and explain how budget terms are derived and uncertainty is assessed (Section 3). After describing the variability measured by satellite (Section 4.1), we detail the results of our budgets based on observations (Section 4.2). We then introduce the inverse methods used to close the budgets within observational uncertainty (Section 5.1) and describe the inverse model results (Section 5.2). We discuss how our results connect to past findings in Section 6 and conclude in Section 7.

2. Budget Framework

2.1. Mass, Volume, and Steric Budgets

The mass budget of our control volume is relatively straightforward because mass is unaffected by sea ice melt and growth. Our mass change term is based on satellite gravimetry data, which measures local changes in ocean mass including sea ice. The mass budget can hence be written as follows:

$$\frac{d}{dt}(\rho V) = M_{OCE} + M_{FW} + M_{SIF}, \tag{1}$$

where $\frac{d}{dt}(\rho V)$ is the rate of change of the mass integrated over the control volume, M represents a net mass flux entering the control volume, and the subscripts represent OCE: ocean, FW: freshwater, SIF: sea ice flux. In other words, mass changes are caused by net ocean, freshwater, and sea ice mass transports. Fluxes are positive into the domain throughout. Our freshwater inputs include river runoff, precipitation minus evaporation and land ice melt.

Because freshwater and sea ice volume fluxes are more readily available than their mass fluxes, and in order to couple our mass and volume budget equations linearly, we cast the freshwater and sea ice mass fluxes as volume fluxes, F, scaled by their densities in our mass budget implementation:

$$\frac{d}{dt}(\rho V) = M_{OCE} + \rho_{FW} F_{FW} + \rho_{SI} F_{SIF}, \tag{2}$$

where we use a freshwater density $\rho_{FW} = 1000$ kg m^{-3} and a sea ice density $\rho_{SI} = 900$ kg m^{-3} (Perovich et al., 2009). The ocean mass flux cannot be cast as simply in terms of its volume flux.

Our volume change term is based on satellite altimeter-based estimates of dynamic ocean topography (DOT), so our control volume includes the ocean volume displaced by sea ice. By Archimedes' principal, a volume V_{SI} of sea ice (with mass $\rho_{SI} V_{SI}$) displaces an equal amount of water such that $\rho_{ML} V_{disp} = \rho_{SI} V_{SI}$, where V_{disp} is the volume of water displaced by sea ice and $\rho_{ML} = 1024.6$ kg m^{-3} is the mixed layer density (we use the mean surface density for the Full Arctic region in the World Ocean Atlas 2023, WOA23, Figure 1 and Figure S1 in Supporting Information S1). Therefore, our volume budget includes the sea ice volume flux into the domain, F_{SIF}, but it is scaled by the ratio of sea ice density and ocean mixed layer density, ρ_{SI}/ρ_{ML}, to account for the displaced ocean volume rather than the full sea ice volume.

We further account for the fact that there is a small change in sea level associated with sea ice melting (Noerdlinger & Brower, 2007). This effect is due to the fact that melted sea ice is generally lower density than the mixed layer water it is displacing. When sea ice melts and becomes freshwater with density ρ_{FW}, the volume of the additional meltwater is $(\rho_{ML} V_{disp})/\rho_{FW}$. So, the small volume contribution from sea ice melt is obtained by scaling the volume flux of sea ice melt, F_{SIM}, by $(\rho_{ML}/\rho_{FW} - 1)$. We note that as $\rho_{ML} > \rho_{FW}$, the melted sea ice volume is larger than the volume that was displaced by the equivalent mass of sea ice. Additionally, Jenkins and Holland (2007) argue that there is a correction required in order to account for the heat required to melt sea ice, which at Arctic Ocean temperatures of about 0°C adds a factor of 0.8.

Taking these considerations into account, the volume budget is

$$\frac{d}{dt}V = F_{OCE} + F_{FW} + \left(\rho_{SI}/\rho_{ML}\right)F_{SIF} + 0.8\left(\rho_{ML}/\rho_{FW} - 1\right)F_{SIM}, \tag{3}$$

where $\frac{d}{dt}(V)$ is the rate of change of the integrated volume and F represents a net volume flux entering the control volume. In other words, changes in the integrated control volume (which is the volume of the ocean including the volume displaced by sea ice), are caused by net oceanic and freshwater fluxes entering the domain as well as sea ice fluxes and sea ice melt, scaled as detailed above.

Finally, we have neglected the effects of external heating and cooling in our volume budget because the Arctic Ocean's density is dominated by salinity changes (see Section 2.2). Over large portions of the Arctic, changes in surface ocean heat content are buffered by sea ice melt and growth and do not lead to significant heat storage (e.g., Steele et al., 2010). We note further that we do account for temperature-driven density changes at the Arctic Straits and hence their contribution to density changes, as we calculate full density fluxes at the Straits. We discuss how temperature changes may influence the interpretation of our budgets further in Section 6.

In this work, we analyze the steric budget, that is, the difference between the volume budget (Equation 3) and mass budget (Equation 2) scaled by ρ_0, as a proxy for an Arctic freshwater budget. The mass scaled by ρ_0 is referred to as mass equivalent throughout and we use $\rho_0 = 1027.8$ kg m^{-3}, which is the mean density of our Full Arctic region in WOA23 (see Figure 1 and Figure S1 in Supporting Information S1). Our steric budget is as follows:

$$\frac{d}{dt}V - \frac{d}{dt}(\rho V)/\rho_0 = \left(F_{OCE} - M_{OCE}/\rho_0\right) + \left(1 - \rho_{FW}/\rho_0\right)F_{FW} \tag{4}$$

$$+0.8\left(\rho_{ML}/\rho_{SI} - 1\right)F_{SIM} + \left(\rho_{SI}/\rho_{ML} - \rho_{SI}/\rho_0\right)F_{SIF},$$

where the LHS of Equation 4 is the steric change term and the steric contributions from ocean fluxes, freshwater fluxes, sea ice melt, and sea ice fluxes are on the RHS. The final term on the RHS of Equation 4 (the sea ice flux term) can be thought of as a correction term for the fact that the satellites measure slightly different control volumes; satellite gravimetry mass values include the mass of water plus the mass of sea ice, whereas satellite altimetry estimates include the volume of water plus the volume of water displaced by sea ice. The sea ice flux term is negligible in our steric budgets. That is, the steric change inferred by the mass and volume satellite products (without the correction term proportional to F_{SIF}) corresponds reasonably well with liquid ocean steric changes (see Sections 2.2 and 4.2).

2.2. Relationship to Freshwater Budgets

The assumption that density varies linearly with salinity, S, has been made to connect steric changes directly with salinity changes in the Arctic Ocean (Armitage et al., 2017; Fukumori et al., 2021; Giles et al., 2012; Morison et al., 2012), that is,

$$\frac{(\rho - \rho_0)}{\rho_0} \approx \beta(S - S_0), \tag{5}$$

where β is the haline contraction coefficient. We check this assumption using in-situ data from WOA23 and the Beaufort Gyre Observing System hydrographic survey data. We find that Arctic changes in density are well-represented by scaled changes in salinity linearizing around mean Arctic properties (Figures S1–S3 in Supporting Information S1).

Given that a linear relationship between density and salinity is a sensible approximation in the Arctic, we can connect steric changes to salinity changes directly. Expanding an expression for local mass change and substituting Equation 5 into it yields

$$\Delta(\rho h) = \rho\Delta h + h\Delta\rho \approx \rho\Delta h + h\rho_0\beta\Delta S,$$

where Δ represents differencing in time, S and ρ are full-depth-averaged and h is the water column height. Further simplifying using the fact that $\beta(S - S_0) \ll 1$ in this parameter space means that we can replace ρ with ρ_0 in front of the height changes, and directly relate steric height changes to changes in salinity:

$$\Delta h - \Delta(\rho h)/\rho_0 \approx - h\beta\Delta S. \tag{6}$$

Salinity changes in the ocean are often described in terms of changes in freshwater content, $\Delta FWC = \Delta\left(\int_{ref}^{sfc}(S_{ref} - S)\,dz\right)/S_{ref}$, where S_{ref} is the reference salinity, and salinity is integrated from the reference isohaline to the surface. ΔFWC can be thought of as having a contribution due to a change in the depth of the bounding reference isohaline plus a contribution due to the salinity change above the reference isohaline. The difference in time of the full-depth integrated salinity ($h\Delta S$) can be directly related to ΔFWC if salinity changes below the bounding reference isohaline have a negligible contribution to $h\Delta S$. If we make the assumption that the salinity changes below the reference isohaline are sufficiently small, we can write Equation 6 as:

$$\Delta h - \Delta(\rho h)/\rho_0 \approx \beta S_{ref}\Delta FWC, \tag{7}$$

which directly connects steric changes to changes in freshwater content.

We test these assumptions and relationships at two repeat hydrographic stations in the Beaufort Gyre (Figure S4 in Supporting Information S1) and find that the scaled full-depth integrated salinity and scaled freshwater content correspond well. We find that they both also match the steric height changes as predicted by Equations 6 and 7. Further, we find good agreement between scaled freshwater content and steric anomaly integrated over the Beaufort Gyre, though the magnitudes of change are not as well matched for the integral as they are for the comparison at the mooring locations (both shown relative to their 2011–2014 mean in Figure 2c).

Morison et al. (2012) deduce an empirical relationship between freshwater content anomalies and steric height anomalies from observations: $\Delta FWC \approx k\left(\Delta h - \Delta(\rho h)/\rho_0\right)$. In our framework, $k = (\beta S_{ref})^{-1}$. Calculating this constant using their reference salinity of 35, yields $k = 37.5$, which agrees reasonably well with their empirically derived $k = 35.6$. In sum, we have derived and tested (Figures 2c and Figure S4 in Supporting Information S1) a relationship for the steric budget and the freshwater budget of the Arctic Ocean that does not rely on any empirical relationships (as in Morison et al., 2012) or two-layer assumptions (as in Armitage et al., 2016; Giles et al., 2012; Lin et al., 2023), providing further justification for our use of the Arctic Ocean's steric budget as an approximation for its freshwater budget.

3. Deriving Budget Terms From Their Data Sources

In this section we describe the data sources for each budget component as well as any additional processing done to calculate the budget terms. We define the Beaufort Gyre region as extending from 65°N to 82°N and 120°W to 180°W (Figure 1). The Full Arctic is defined as north of all Arctic Straits (Bering Strait, Davis Strait, Fram Strait, and the Barents Sea Opening), but does not include the Canadian Arctic Archipelago as satellite altimetry data are not available in that area (Armitage et al., 2016). Unlike Armitage et al. (2016), we do include Baffin Bay in our study region, as Davis Strait is one of our boundaries. Unless otherwise noted, all budget components are integrated over both the Beaufort Gyre and Full Arctic regions. We describe the uncertainty in each data source. If a percentage uncertainty is not given, we convert local uncertainties to total budget term uncertainties by multiplying by the appropriate surface area. When integrating budget terms in time, we sum the errors cumulatively (not in quadrature) to allow for systematic error. Note that uncertainties for the volume and mass storage terms are shown in Figures 4–7, but they do not factor into our inverse model closure (Section 5).

3.1. Volume Change From Satellite Altimetry

Volume changes $\left(\frac{d}{dt}V\right)$ are estimated using monthly DOT products derived specifically for the Arctic from satellite radar altimetry. The first product covers 2003–2014 and is derived from the Envisat and Cryosat-2 satellites (Armitage et al., 2016). The data are masked within 10 km of land and smoothed using a Gaussian convolution filter, with a standard deviation of 100 km and a radius of 3 standard deviations. It is provided on a 0.25° grid. The second product covers the Cryosat-2 era from 2011 to 2020, uses the same methodology, and is

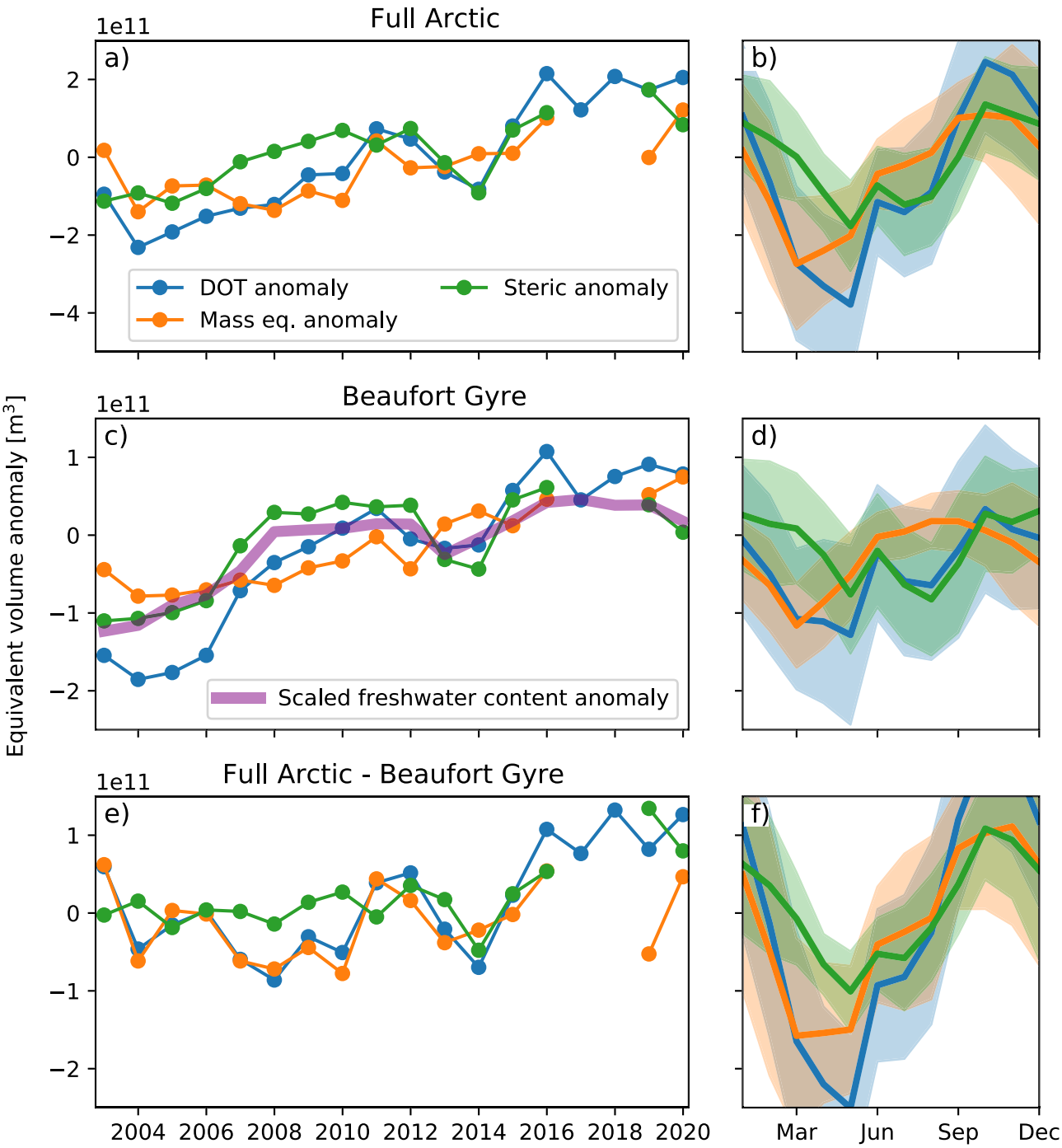

Figure 2. Annual mean (a, c, e) and seasonal climatologies (b, d, f) of the spatially integrated dynamic ocean topography anomaly, mass equivalent anomaly and their difference, the steric component, for the Full Arctic and Beaufort Gyre regions defined in Figure 1, as well as the difference between the two regions. Scaled Beaufort Gyre freshwater content anomaly from hydrography as defined in Section 2.2 is shown in panel (c). The seasonal climatologies are shown with envelopes of ±1 standard deviation.

available on a 20 km grid. We use the "smoothed" DOT product provided from 2014 onward to extend the Armitage et al. (2016) product. In order to merge the two products, we remove the mean from January 2011 to December 2014 from both. A comparison of the products including their period of overlap is in Figure S5 in Supporting Information S1. Data based on the Envisat altimeter have a "pole hole", where no data are available north of 81.5°N. For consistency over time, we only use data south of 81.5°N during the entire study period. From

2011 to 2020, the total volume integrated over the full Arctic with and without data in the "pole hole" have a correlation of 0.99 and the ratio of their standard deviations is 1.02. This is consistent with the analysis of Armitage et al. (2016), who similarly leave out the "pole hole" for their entire study period. Following Armitage et al. (2016), we use an uncertainty of 1.1 cm in the monthly DOT, which is calculated from differences in DOT at satellite crossover locations, lead/open ocean bias, inter-satellite bias, and uncertainty associated with neglecting data north of the "pole hole."

3.2. Mass Equivalent Change From the GRACE Satellite

Mass equivalent changes $\left(\frac{d}{dt}(\rho V)/\rho_0\right)$ are derived from Gravity Recovery and Climate Experiment (GRACE) and GRACE Follow-On satellite data. We use the Jet Propulsion Laboratory processed "mass concentration block" (mascon) solutions Release 06.1 Version 03 (Watkins et al., 2015) with the Coastal Resolution Improvement (CRI) filter, which reduces signal leakage across coastlines (Wiese et al., 2016). Although data are available on a 0.5° grid, the nominal resolution is 3° as this is the size of the individual mass concentration block. The data are monthly and there is reliable data coverage from 2004 to 2010. However, starting in 2011 data gaps of one and two months become common until GRACE data ceased to be available for this region in August 2017. The GRACE Follow-On mission started reporting data in June 2018. The GRACE data were interpolated to the altimeter time grid (15th of each month) and the gaps shorter than three months were interpolated over linearly. We fill the longer gap between missions with the climatology from 2004 to 2010 (when the data are most reliable) for our budget analysis but leave out the gap between GRACE misions in the analysis presented in Figure 2. The original and interpolated ocean mass anomaly data integrated over the Full Arctic region are shown in Figure S6 in Supporting Information S1. Finally, we subtract the scaled ERA5 monthly global mean sea level pressure anomaly (Armitage et al., 2016). We find a seasonal cycle of global mean sea level pressure of only about 0.3 cm from ERA5, compared to the 0.8 cm cited by Armitage et al. (2016) based on ERA-Interim. In order to be consistent with the volume anomaly calculations from satellite altimetry, we subtract the mean from 2011 to 2014 from our ocean mass anomaly time series. We also leave out all data north of the 81.5°N "pole hole" following Armitage et al. (2016). We use an uncertainty in mass equivalent height anomaly of 1.6 cm, which includes both a literature estimate and the error associated with neglecting data north of the "pole hole" (Armitage et al., 2016; Chambers & Bonin, 2012).

3.3. Freshwater Fluxes

In our framework, freshwater volume fluxes (F_{FW}) are the sum of river runoff, precipitation minus evaporation, and land ice contributions (Figure 3). The contribution from relatively fresh Pacific Waters is included in our F_{OCE} and M_{OCE} terms. River runoff is the primary component of the freshwater flux for the Full Arctic region, followed by net precipitation and then land ice contributions. In the Beaufort Gyre, the split between river runoff and net precipitation is more even and land ice does not directly contribute (no green line in Figure 3b). The differences between the total freshwater fluxes estimated from different data products are discussed in the subsections below. Given this spread as well as the spread reported in the literature (see below), we estimate an uncertainty on our freshwater flux of 20%. Our uncertainty is larger than the Haine et al. (2015) estimate of 10%, as we consider monthly means and they consider decadal averages.

3.3.1. Precipitation Minus Evaporation

We use monthly total precipitation and evaporation data from the European Centre for Medium-Range Weather Forecasts (ECMWF) fifth generation reanalysis (ERA5) (Copernicus Climate Change Service, 2017; Dee et al., 2011) available on a 1/4° grid. Uncertainties in precipitation minus evaporation are high due to scarce observations and the spread between reanalysis products is significant (Barrett et al., 2020; Bintanja et al., 2020; Boisvert et al., 2018). There is no clear best reanalysis product to use based on comparisons with observations, but ERA5 is the recommended precipitation product because of its resolution and because it will be continued into the future (Barrett et al., 2020).

3.3.2. River Runoff and Land Ice Contributions

We estimate the sum of river runoff and land ice contributions using the Japanese 55-year atmospheric reanalysis 1/4° resolution data set for driving ocean-sea-ice models (JRA55-do) (Figure 3; Tsujino et al., 2018). The river

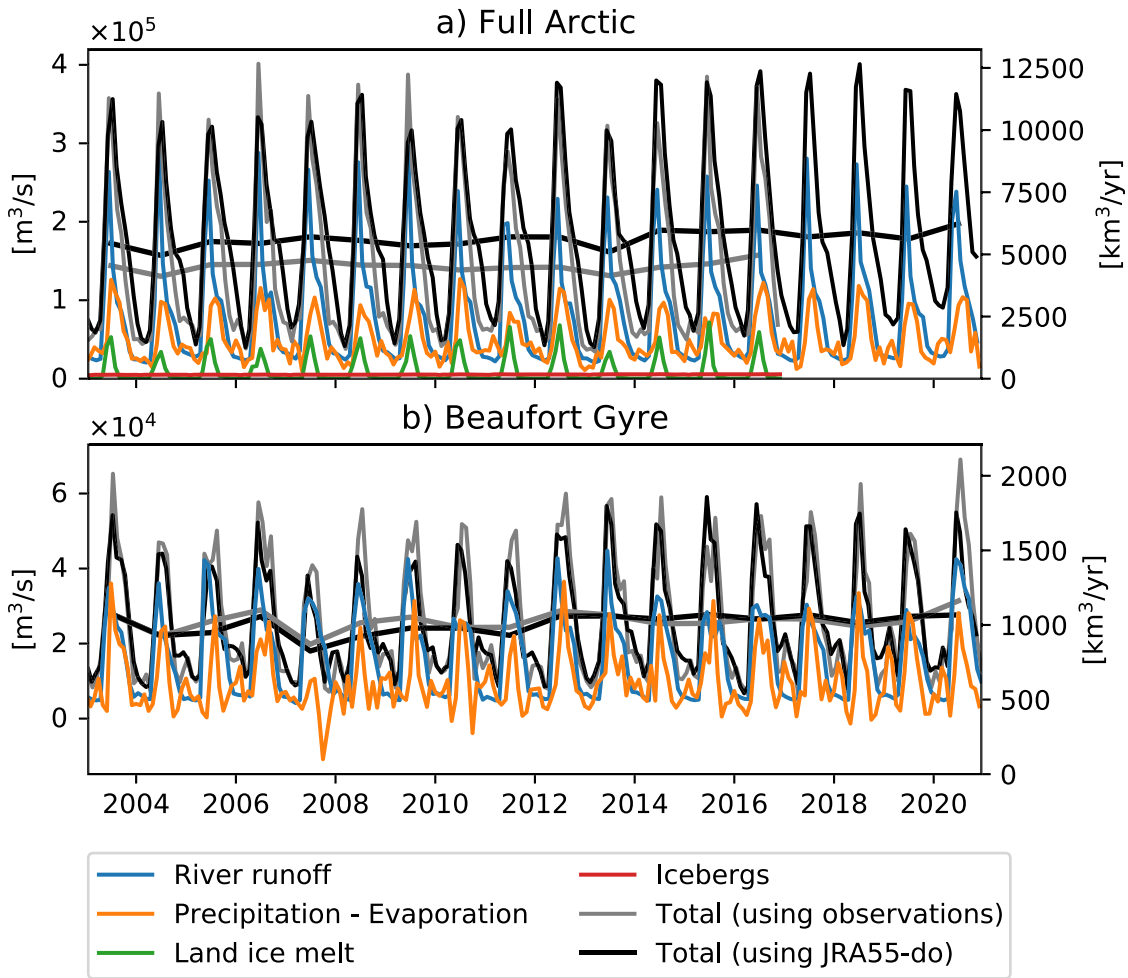

Figure 3. Observed monthly freshwater fluxes and the contributing sources in each budget region. The thick black and gray lines are annual means.

runoff portion of this product is the output of the CaMa-flood global river routing model calibrated against reference data for the major rivers (Suzuki et al., 2018). The land ice runoff from Greenland and the surrounding islands is from Bamber et al. (2018a, 2018b), which is based primarily on satellite observations and regional drainage models. JRA55-do incorporates these liquid fluxes at monthly time steps from 1958 to 2016. After 2016, the 2012–2016 climatology is used. We show the Bamber et al. (2018a, 2018b) liquid land ice runoff and solid ice fluxes for reference (Figure 3). These are from the pre-defined basins numbered 29, 30, 83, 84, and 86 in the data set, which, when summed, correspond to the sum of the Baffin Bay, Arctic, and Barents Sea regions. The solid ice fluxes (icebergs) are not included in our budget as it is an uncertain and small term for this region.

Total river runoff calculated from the Arctic Great Rivers Observatory discharge data (McClelland et al., 2023) is also shown for reference (Figure 3). Our river runoff estimate for the Full Arctic region includes all rivers in the data product; our estimate for the Beaufort Gyre region is the sum of the Mackenzie and Yukon rivers. Data gaps of up to 90 days were filled using linear interpolation. If river discharge records had longer gaps, the river record was replaced with a climatology comprised of the mean seasonal cycle from all available data for that river from January 1980 to January 2022. The uncertainty associated with using these climatologies was found to be about 40% (the ratio of the mean of the total standard deviation for these rivers to their mean annual flux during observed years). Rivers for which a climatology was used account for 14% of the total discharge into the Full Arctic region, so that the uncertainty added to the total by filling in gaps with climatology is 5%. No filling using climatology was necessary for the Mackenzie and Yukon rivers that flow into the Beaufort Gyre region.

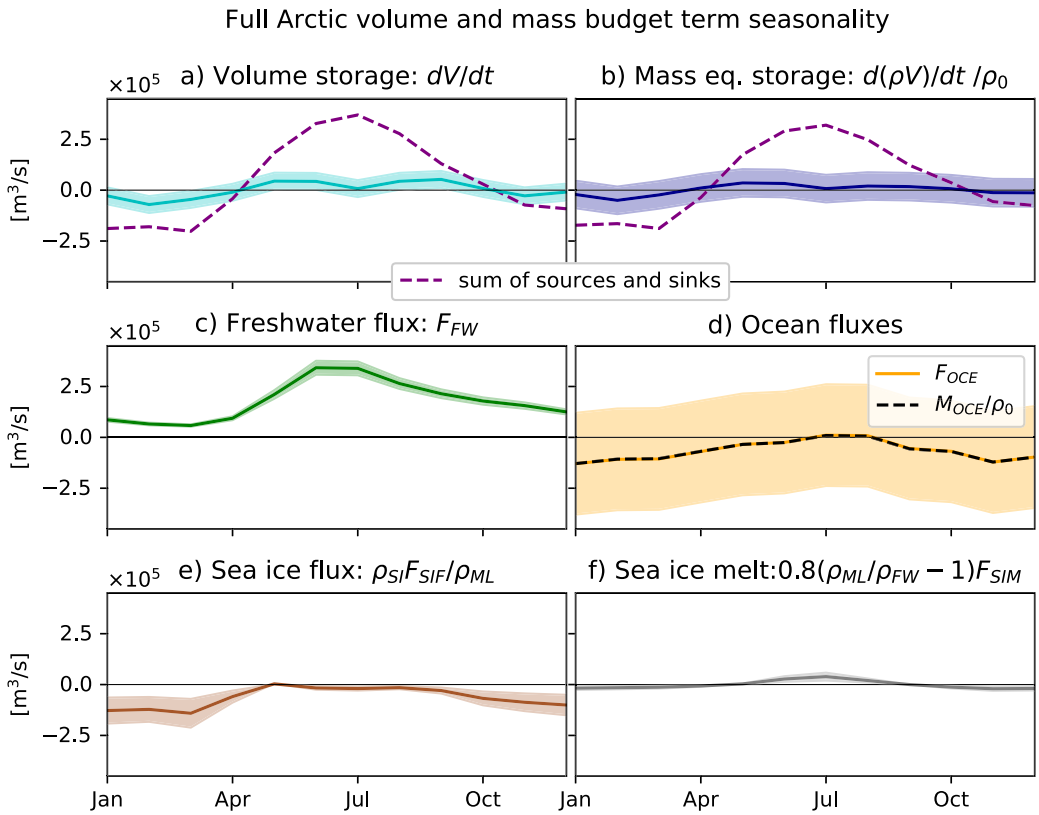

Figure 4. Seasonal climatology of observation-based volume and mass budget terms for the Full Arctic region, with shading representing their uncertainty. The purple dashed lines in panels (a) and (b) are the sum of the source and sink terms for the volume and mass, respectively.

The total freshwater fluxes calculated using JRA55-do versus using the Arctic Great Rivers Observatory and Bamber et al. (2018a, 2018b) data directly differ by about 1000 km^3/yr for the Full Arctic region (Mean values from 2003 to 2016: 5550km^3/yr vs. 4520km^3/yr; Figure 3). This difference stems from the river runoff products (Mean values from 2003 to 2016: 3680km^3/yr vs. 2610km^3/yr), which are known to have a wide spread depending on the data source (Winkelbauer et al., 2022). The total freshwater fluxes for the Beaufort Gyre region from the two different product combinations agree more closely (Mean values from 2003 to 2016: 780km^3/yr vs. 810km^3/yr). Our reconstruction based on the Arctic Great Rivers Observatory data is likely biased small for the Full Arctic because it only includes the (gauged portions of) major rivers. We elect to use the total based on the JRA55-do product as it agrees more closely with other estimates (Stadnyk et al., 2021; Winkelbauer et al., 2022).

3.4. Ocean Fluxes From Arctic Strait Ocean Fields

Our ocean volume and mass fluxes (F_{OCE} and M_{OCE}, respectively) are based on the Arctic Strait ocean fields presented by Tsubouchi et al. (2023). Their monthly mean property and transport fields are inverse model solutions generated in the context of mass, salt, and heat budgets for the Arctic Ocean to the north of the Arctic Straits from October 2004 to April 2010. The fields are based primarily on moored arrays as well as some repeat hydrographic sections. In this analysis, we use repeating seasonal climatologies of the net volume and mass transports into the Arctic to represent F_{OCE} and M_{OCE} for our Full Arctic region.

The net volume transport into the Arctic in the Tsubouchi et al. (2019) product is constructed to balance surface freshwater fluxes, which are initialized as their time mean and allowed to vary significantly by the inverse model. Their surface freshwater flux term is meant to conceptually include storage. So, they do not attempt to recreate true freshwater flux variability, but instead aim to produce the oceanic fluxes most consistent with in situ observations. We expect the ocean fluxes to be altered by our inverse model budget closure due to the differences between our frameworks.

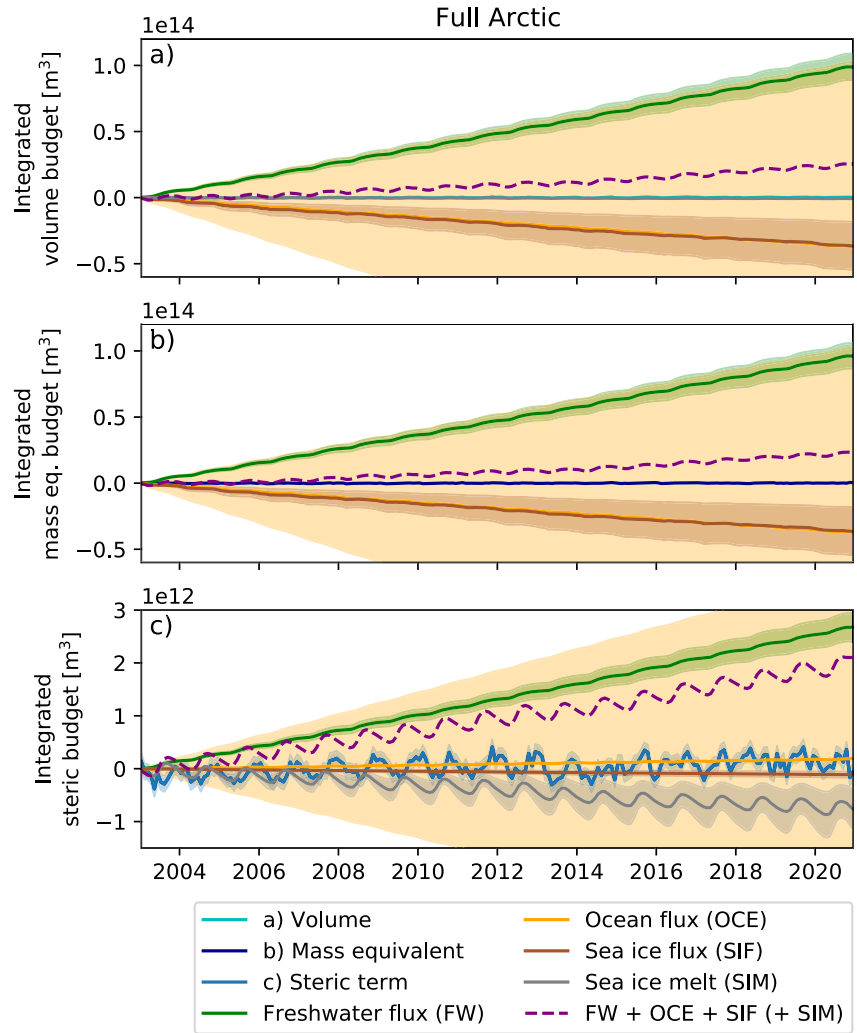

Figure 5. Observation-based time integrated volume, mass equivalent, and steric budgets for the Full Arctic region. Each term is shown with shading corresponding to observational uncertainty.

There is significant uncertainty in the ocean volume flux, particularly because of large unobserved regions over Belgica Bank (the western shelf of Fram Strait) and north of Bear Island in the Barents Sea Opening (Tsubouchi et al., 2023). Additionally, the month-to-month transport variability through each of the Straits is O(5 Sv). We hence estimate the uncertainty in the total volume transport, F_{OCE}, and mass equivalent transport, M_{OCE}/ρ_0 to be 0.25 Sv each month.

The net volume fluxes we calculate from the gridded Tsubouchi et al. (2019) product are larger (less negative) than those they report separately (see Figure S7 in Supporting Information S1). This is a known issue in calculating the volume transports from the gridded velocities, stemming from using inverse modeling software to calculate transports (see the supplementary materials of Tsubouchi et al. (2018)). The difference is about 20 mSv, which would normally be a very small difference for oceanographic volume transports. However, it is not a negligible difference when considering the net volume transport through all the Straits. The details of the ocean flux initial conditions do not influence the inverse model solution, and our prescribed uncertainty is much larger than this difference, so our conclusions are robust to these issues.

Estimating the ocean flux in and out of the Beaufort Gyre region is not feasible given the current data constraints, so we estimate $F_{OCE} = 0$ Sv and $M_{OCE}/\rho_0 = 0$ Sv for the Beaufort Gyre region as a first guess and allow a 0.25 Sv uncertainty in both as we do for the Full Arctic region.

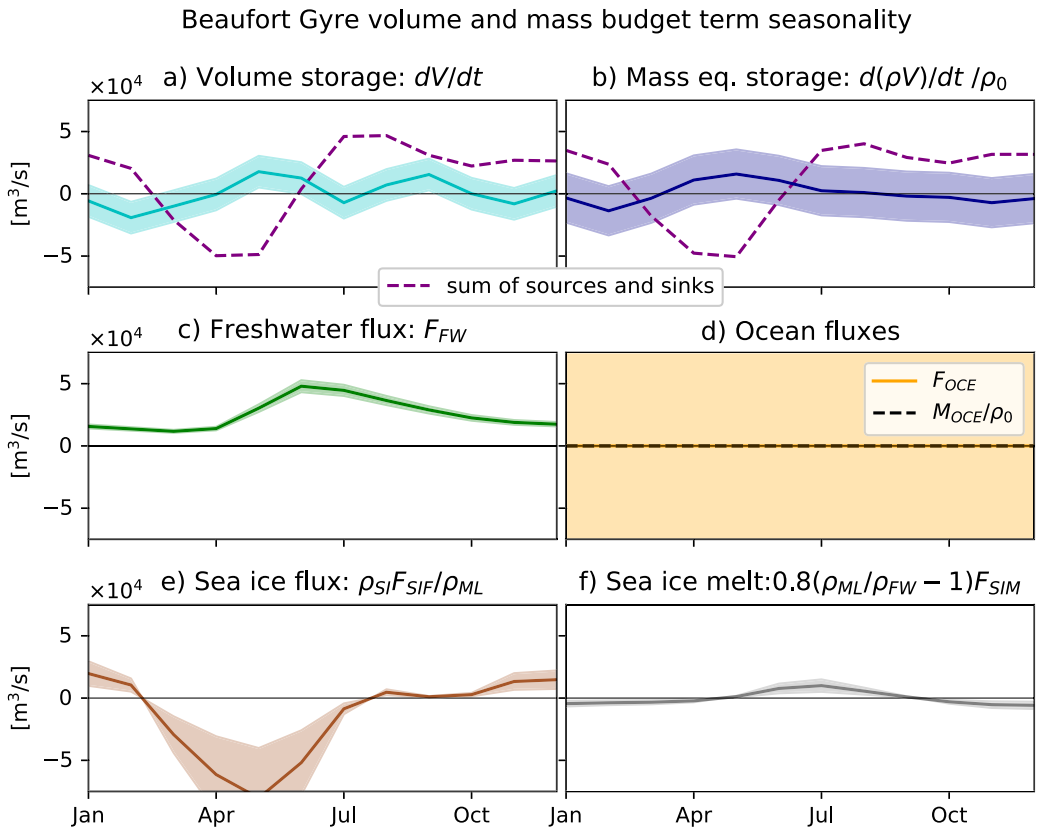

Figure 6. Seasonal climatology of observation-based volume and mass budget terms for the Beaufort Gyre region, with shading representing their uncertainty. The purple dashed lines in panels (a) and (b) are the sum of the source and sink terms for the volume and mass, respectively.

3.5. Sea Ice Fluxes and Melt Rates From PIOMAS

Sea ice volume fluxes (F_{SIF}) and sea ice melt (F_{SIM}) are calculated from the Pan-Arctic Ice-Ocean Modeling and Assimilation System (PIOMAS) model output. PIOMAS is a coupled ice-ocean model that assimilates sea ice concentration (Lindsay & Zhang, 2006; Zhang & Rothrock, 2003). We use the sea ice advection term (advect) and sea ice production (iceprod) and integrate each over both budget regions. The PIOMAS ice production is multiplied by negative one to get our sea ice melt term, F_{SIM}. PIOMAS has undergone extensive validation against in situ thickness observations and is used widely in sea ice research as satellite observations provide sea ice area much more reliably than sea ice thickness (Babb et al., 2022; Howell et al., 2016; Moore et al., 2019); satellite sea ice thickness is a relatively nascent measurement and is limited to periods of sea ice growth (Laxon et al., 2013). Haine et al. (2015) report freshwater loss in multiyear ice from PIOMAS and indicate that it agrees relatively well with the satellite-based estimates of Kwok et al. (2009) and Laxon et al. (2013). Schweiger et al. (2011) assessed PIOMAS errors in detail and found that although correlations with in situ data are high, biases of up to about 0.3 m are not uncommon. In an auxiliary analysis, we similarly find reasonable agreement between monthly sea ice thickness estimates from PIOMAS (heff) and upward looking sonar measurements on Beaufort Gyre Observing System moorings (Krishfield et al., 2014) (Figure S8 in Supporting Information S1), but confirm that biases on that order are common. Additionally, we note that there is sometimes a bias in the seasonality, with PIOMAS showing sea ice thickening one or 2 months earlier than the direct observations.

The total sea ice flux into the Arctic from PIOMAS agrees well with the flux across Fram Strait as observed by moored upward looking sonar measurements reported in Sumata et al. (2022) (Figure S9 in Supporting Information S1). Note that the flux out of Fram Strait is known to dominate the sea ice flux out of the Arctic. Sumata et al. (2022) estimate errors of about 30% in decadal averages of Fram Strait sea ice volume flux and Haine et al. (2015) state that freshwater storage as sea ice is the least constrained term of the Arctic freshwater budget. We use a generous uncertainty of 50% for all sea ice volume flux and melt rate terms.

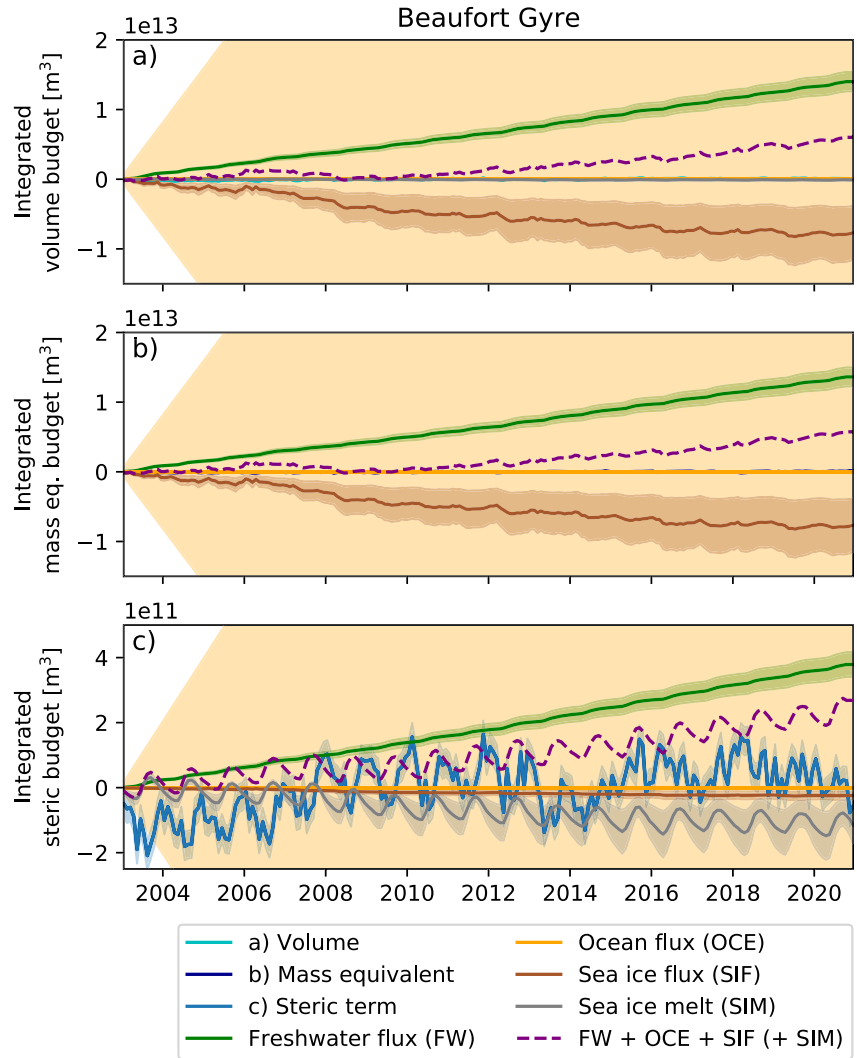

Figure 7. Observation-based time integrated volume, mass equivalent, and steric budgets for the Beaufort Gyre region. Each term is shown with shading corresponding to observational uncertainty.

4. Observation-Based Results

4.1. Volume and Mass Variability From Satellite

The predominant spatial patterns of Arctic DOT anomaly (Figure 1a) are a maximum in the Beaufort Gyre and minimum in the Greenland Sea, as presented by Armitage et al. (2016). The mass equivalent patterns mirror those of the DOT within our Full Arctic region, and the coarse resolution of the GRACE satellite is apparent (Figure 1b). The magnitude of the mass equivalent anomaly is much smaller than the total DOT, particularly in the Beaufort Gyre region, implying that the doming in the Beaufort Gyre is due to its low density, that is, that the steric component of the DOT is important. The patterns are qualitatively similar when the data sets are extended through 2020 (not shown).

The DOT, mass equivalent, and the steric component exhibit pronounced long-term changes in the Full Arctic region (Figure 2a). The steric anomaly increased from 2003 to 2012, then dropped in 2013 and 2014, and increased again until 2020. The increase in the first part of the record is dominated by changes in the Beaufort Gyre region, which have been reported on extensively (Figure 2c; Armitage et al., 2016; Giles et al., 2012, p. 435; Proshutinsky et al., 2009). There is virtually no change in steric anomaly in the region of the Arctic outside the Beaufort Gyre before 2013 (Figure 2e). The decrease in 2013 is seen in the Beaufort Gyre only and in 2014 it is

seen primarily outside the Beaufort Gyre, suggesting that this decline is associated with a freshwater anomaly leaving the Beaufort Gyre and transiting through the rest of the Arctic. Finally, the increase in the steric anomaly after 2014 occurs both within and outside the Beaufort Gyre. In fact, after 2016, the steric anomaly increases outside the Beaufort Gyre exclusively, although the steric anomaly is relatively stable in the Beaufort Gyre (Lin et al., 2023; Timmermans & Toole, 2023). We note, however, that there were transitions between satellite products in the later part of the record, so the true uncertainty is likely higher during this time period.

The seasonal cycles of DOT, mass equivalent, and the steric component are similar in magnitude to the long term changes (Figure 2). The DOT, mass equivalent, and steric anomalies have minima in the spring and maxima in the fall as well as a weaker maximum in June that is most significant in the Beaufort Gyre, which has been noted previously and associated with river runoff (Armitage et al., 2016; Peralta-Ferriz & Morison, 2010; Proshutinsky et al., 2009). The seasonal variability we find is unchanged relative to that reported by Armitage et al. (2016), who describe the seasonal patterns in greater detail.

4.2. Budgets From Observations

4.2.1. Full Arctic

Seasonality dominates the variability of all Full Arctic volume and mass budget terms (Figure S10 in Supporting Information S1). The variability of the dominant source and sink terms are in phase: freshwater flux peaks in June and the ocean and sea ice flux out of the Arctic is weakest in summer (Figure 4). The sea ice melt term, which only enters in the volume budget, also peaks in summer, but is much smaller than the other source and sink terms. The sum of the source and sink terms is greater in magnitude than the volume storage and mass equivalent storage measured by satellite, but their variability is in phase, with volume and mass increases in summer and decreases in winter (Figures 4a and 4b). The disagreement is likely due to errors in the ocean fluxes as these have the largest uncertainty, but may also be related to an underestimate of the total seasonal cycle inferred from the satellite data as we discuss further in Section 6.

The time-integrated mass and volume budgets for the Full Arctic show a dominant balance between inflow of freshwater and outflow of sea ice and ocean water (Figures 5a and 5b). The sea ice melt term is too small to discern from zero in Figure 5a. The sum of the source and sink terms predicts an unrealistic net increase of volume and mass (purple lines in 5a,b). However this net increase is small compared to the large uncertainty in the ocean flux, which is reflected by the dominance of the orange shading in Figure 5.

The integrated steric term, which can be thought of as corresponding to freshwater content, is larger relative to the integrated source and sink terms than the volume and mass are in the time-integrated budget (Figure 5c). The sum of the integrated source and sink terms (purple) predict an increase that is largely driven by the inflowing freshwater fluxes and is significantly greater than that inferred from satellite data (blue). There is a negative contribution from the sea ice melt term, which comes from the fact that there is net sea ice growth in the Arctic (and an associated densification). The seasonal cycle of the integrated steric term is relatively well explained by the seasonality in the sea ice melt term. There is a small positive contribution from the ocean fluxes, but this is likely an artifact of how they are calculated from the gridded product (see Section 3.4). This illustrates how sensitive these budgets are to the details of the calculation of the ocean flux in particular. In reality, we would expect the ocean contribution to be negative as the outflows are fresher and lighter in the net than the inflows (Tsubouchi et al., 2023).

4.2.2. Beaufort Gyre

The volume and mass budget terms for the Beaufort Gyre are similarly dominated by seasonality (Figure 6 and Figure S11 in Supporting Information S1). We do not have an observation-based estimate for the ocean fluxes into the Beaufort Gyre region, so they are taken to be zero. The sea ice flux estimated from PIOMAS shows export from the Beaufort Gyre in late spring (with considerable interannual variability) and sea ice convergence in the Beaufort Gyre in winter. As for the Full Arctic, the freshwater flux peaks in the summer and the sea ice melt is a small source term in the volume budget. The seasonality in the sum of the source and sink terms does not match the seasonality in the volume and mass equivalent storage terms (Figures 6a and 6b), which is not too surprising

given that the ocean fluxes have not been accounted for. At the same time, the magnitude of their variabilities is better matched than it is for the Full Arctic seasonal budget.

The Beaufort Gyre's time-integrated volume and mass budgets are predominantly a balance between freshwater inflow and sea ice export (Figures 7a and 7b). The sum of the source and sink terms shows a net inflow to the Beaufort Gyre, which is within the estimated uncertainty of the ocean flux contribution and implies a net outflow of ocean water to balance the volume and mass budgets.

As for the Full Arctic, freshwater inflow is a significant positive term in the Beaufort Gyre's time-integrated steric budget, and the sea ice melt term is negative (Figure 7c). The sum of the integrated source terms (purple) is consistent with freshwater accumulation in the Beaufort Gyre, but it has otherwise poor correspondence with the steric term inferred from satellite data (blue). In particular, the magnitude of the seasonal and interannual variability in the sum of the integrated source terms is weaker than that estimated from satellite.

5. Budget Closure Using Inverse Methods

5.1. Inverse Model Framework

We use inverse methods to close the coupled volume and mass budgets in a way that acknowledges the uncertainty in each budget term, similar to the approach used in Le Bras et al. (2021). Our starting point is the matrix form of the volume and mass budget equations:

$$\mathbf{A}(\bar{\mathbf{x}} + \mathbf{x}') = \mathbf{0}, \tag{8}$$

where $\mathbf{A}$ contains the volume and mass budget equation operators (Equations 2 and 3),

$$\mathbf{A} = \begin{pmatrix} -1 & 0 & 1 & 0 & 1 & \rho_{SI}/\rho_{ML} & 0.8(\rho_{ML}/\rho_{FW} - 1) \\ 0 & -\rho_0 & 0 & 1 & \rho_{FW} & \rho_{SI} & 0 \end{pmatrix},$$

and $\bar{\mathbf{x}}$ is a vector that holds the initial observation-based estimates of the unknowns, which are described in Sections 2 and 3 and shown in Figures 4–7 (full time series in Figures S10 and S11 in Supporting Information S1), that is,

$$\bar{\mathbf{x}} = \left(\frac{d}{dt}V \quad \frac{d}{dt}(\rho V)/\rho_0 \quad F_{OCE} \quad M_{OCE} \quad F_{FW} \quad F_{SIF} \quad F_{SIM} \right)^T.$$

We saw in Section 4.2 that the budgets do not close using our observation-based estimates, so we are solving for $\mathbf{x}'$, the vector of the minimum deviations from these that enable closure of both the mass and volume budgets. To do this, we use a weighted inverse model following Wunsch (1996) and recast Equation 8 as follows:

$$\left(\mathbf{W^{-1}AE}\right)\left(\mathbf{E^{-1}x'}\right) = -\mathbf{W^{-1}A}\bar{\mathbf{x}}, \tag{9}$$

where $\mathbf{W}$ is the row weighting matrix, which normalizes the mass budget equation by ρ_0^{-1} so that it is the same order as the volume budget equation and $\mathbf{E}$ is a diagonal matrix with entries corresponding to the observational uncertainty in each budget term. The notable exception to this is that we assign the volume and mass storage terms, $\frac{d}{dt}V$ and $\frac{d}{dt}(\rho V)/\rho_0$, zero uncertainty because we are seeking to explain these observed storage changes.

We solve the inverse model equations using a singular value decomposition of $\left(\mathbf{W^{-1}AE}\right)$ such that its pseudo-inverse is $\left(\mathbf{V}\,\mathbf{\Lambda^{-1}}\,\mathbf{U^T}\right)$, where $\mathbf{U}$ and $\mathbf{V}$ are square eigenvector matrices and $\mathbf{\Lambda}$ is a rectangular matrix with eigenvalues on the diagonal. The solution to the weighted equations can hence be written, $\mathbf{x'} = -\mathbf{E}\left(\mathbf{V\Lambda^{-1}U^T}\right)\mathbf{W^{-1}A}\bar{\mathbf{x}}$. We solve this equation at each monthly time step independently and present the initial conditions plus the deviations required to close the budgets $(\bar{\mathbf{x}} + \mathbf{x}')$ as our solutions.

5.2. Inverse Model Results

The inverse model minimally adjusts all budget source terms in proportion to their uncertainty in order to explain the observed mass and volume storage changes, and consequently, the steric changes. The integrated steric budgets based on the inverse model solutions are more meaningful than those from the observations as they are based on budgets that conserve volume and mass, and can be thought of as closed freshwater content budgets.

The ocean mass and volume fluxes have the largest uncertainty and are hence the most adjusted terms in both the Full Arctic and Beaufort Gyre inverse model solutions (difference between dashed and solid orange lines in Figure 8). The other significant source and sink terms in the steric budget have smaller uncertainties than the ocean fluxes and are only very weakly adjusted by the inverse model (small difference between the dashed and solid green and gray lines in Figure 8).

The ocean fluxes in both solutions are adjusted such that their steric contributions account for any seasonal and interannual variability necessary to close the mass and volume budgets. In the Full Arctic steric budget, the ocean fluxes are a persistently negative term, implying that the ocean is a net sink for freshwater fluxes. This is consistent with our understanding that the net inflows to the Arctic are saltier (and denser) than the fresh (and light) outflows (Tsubouchi et al., 2023).

In the Beaufort Gyre, the ocean flux term solution has much more interannual variability compared to the other source and sink terms. In particular, the patterns of freshwater accumulation (2006–2008 and 2014–2016) and release (2012–2014 and 2018–2020) are linked to ocean flux changes. This is consistent with our understanding that oceanic convergence of freshwater drives Beaufort Gyre freshwater content changes (Proshutinsky et al., 2009). Superimposed on these decadal variations is an overall negative contribution from the ocean fluxes, implying that there is a persistent overall loss of freshwater (decrease in density) that is attributable to ocean fluxes.

To examine which source and sink terms dominate the interannual steric changes in the inverse model solution in more detail, we break down the contribution of the primary source and sink terms to the year-to-year steric changes. We remove the mean over the full time series from each of the source and sink terms, so that the changes from year-to-year are highlighted. We find that the oceanic contribution can explain most of the interannual variability in both regions (orange bars are the dominant contribution to the black bars in Figures 9b and 9c).

The Full Arctic steric changes are dominated by changes in the Beaufort Gyre (Figure 9a) and the interannual variability in the ocean fluxes for the Full Arctic and Beaufort Gyre budgets generally co-vary. For example, when there is a freshwater accumulation in the Beaufort Gyre (2006–2008 and 2014–2016) there is also freshwater convergence in the Full Arctic. This could be accounted for by atmospheric forcing patterns, that is, when there is a stronger Beaufort High, associated atmospheric patterns drive increased flow through Bering Strait, or weaker outflow of relatively fresh ocean water through Fram or Davis Strait.

The change in ocean volume flux required to account for these interannual steric changes are on the order of 50 mSv (Figure 9d), which are much smaller than we can measure using oceanographic moorings. In fact, the size of the adjustments are on the same order as the error incurred when calculating the net transport out of the Arctic using the gridded Tsubouchi et al. (2019) data set versus the net transport calculated by their inverse modeling software (see Section 3.4). In the Beaufort Gyre, there is a convergent ocean volume flux of about 25 mSv in 2007 and 2008 associated with freshwater accumulation, whereas the ocean volume flux is otherwise generally divergent. The ocean volume flux for the Full Arctic region is always negative and increases in magnitude toward the end of the record when there is a declining steric anomaly (freshwater loss).

Associating the ocean volume flux (Figure 9d) with the ocean contribution to the steric budget (Figures 9b and 9c) is not straightforward as the latter is the difference between the volume transport and the mass equivalent transport, which largely mirrors the volume transport (not shown). In other words, changes in density also have to be considered. For the Full Arctic budget, the net ocean flux is the difference between flows through all the Straits, each of which have different density, temperature, and salinity signatures. In the Beaufort Gyre the net ocean flux is the difference between Ekman and eddy fluxes, which are less well-defined and topographically constrained than the flows through the Straits, making them more difficult to quantify and compare across observations and models.

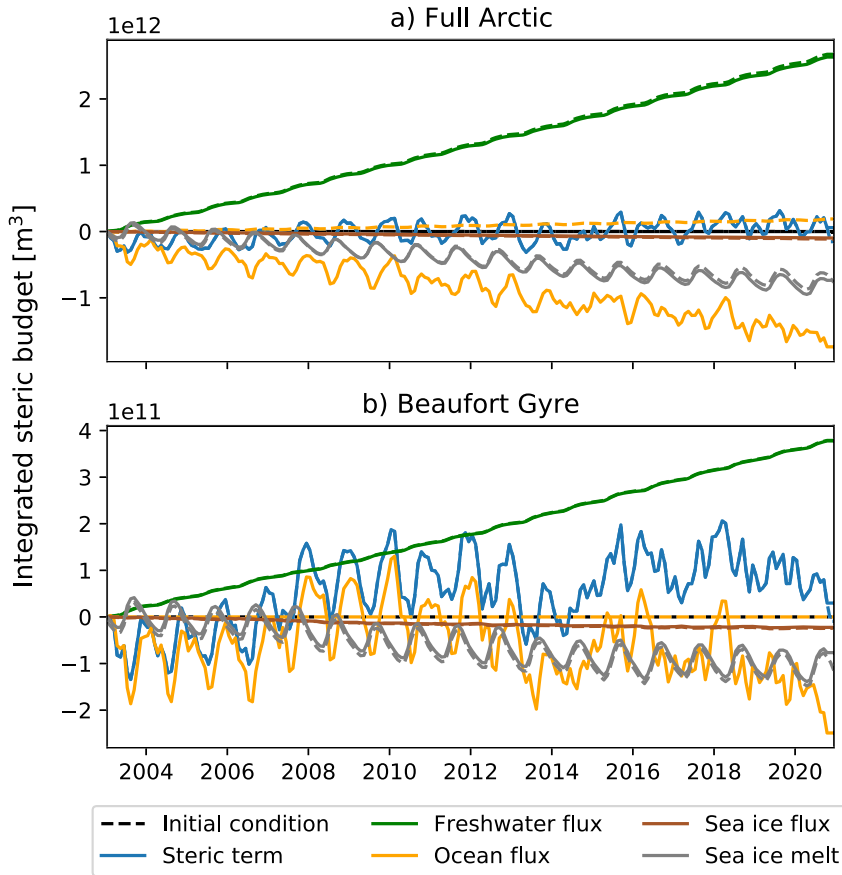

Figure 8. Integrated steric budget initial conditions (dashed lines) and inverse model solutions (solid lines) for (a) the Full Arctic and (b) the Beaufort Gyre regions. Initial conditions are repeated from Figures 5c and 7c, but uncertainty envelopes are left out for readability.

6. Discussion

6.1. Comparing Freshwater Changes to Other Studies

Our analysis of satellite observations shows that there was an increase in steric height of the Beaufort Gyre, which was roughly equivalent to the increase in steric height over the Full Arctic (Figures 2 and 9a). This is seemingly in conflict with studies that highlighted the compensation of freshwater between the Beaufort Gyre and the rest of the Arctic in the 2000s. For example, Morison et al. (2012) state, based on an analysis of steric height, that the freshwater increase in the Beaufort Gyre coincided with a "nearly negligible increase in average Arctic Ocean freshwater." We find a similar result when we calculate domain averages instead of the spatially integrated quantities presented in Figure 2. That is, we also find a negligible increase in the steric height of the Full Arctic (Figure S12 in Supporting Information S1) because the negligible changes in most of the Arctic dominate the calculation, that is, the Beaufort Gyre freshwater changes are limited to a relatively small area. It is worth noting that Baffin Bay is not included in Morison et al. (2012). McPhee et al. (2009) also highlighted redistribution of Arctic freshwater as a source for Beaufort Gyre freshwater increase, but estimated that freshwater decline in the areas outside the Beaufort Gyre was about one quarter the size of the increase.

To compare the size of the freshwater increases we find in the Full Arctic and the Beaufort Gyre directly to other studies, we use the freshwater content scaling derived in Section 2.2. The scaled freshwater content from annual hydrographic observations taken in the Beaufort Gyre agree well with the steric anomaly measured (Figures 2c and 9a). The primary discrepancy is that the satellite steric anomaly decreases more in 2014 than the scaled freshwater content from hydrography. This is likely not entirely due to differences in sampling time (hydrographic surveys occur in summer and we show annual mean steric heights); we find larger differences between

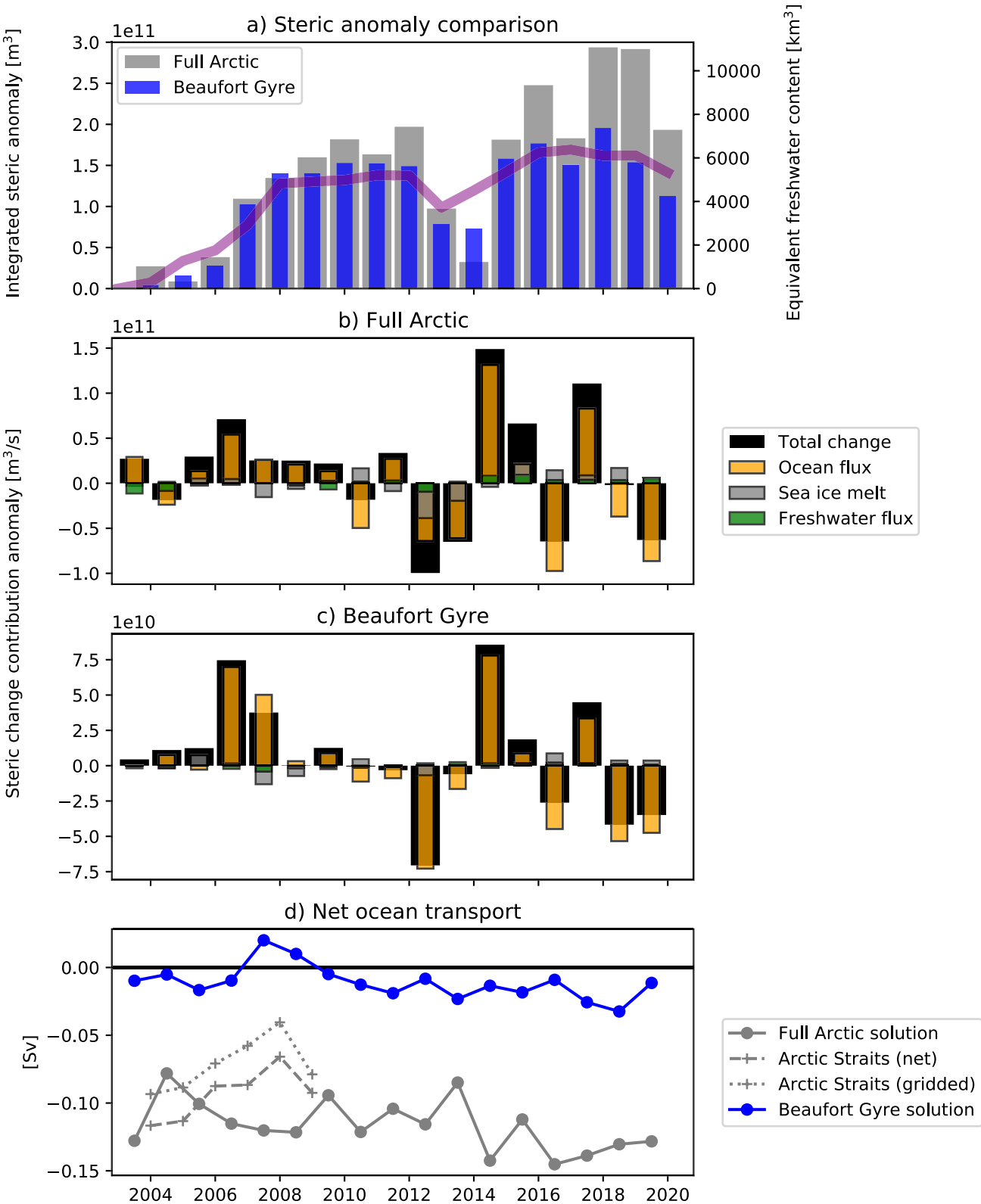

Figure 9. (a) Spatially integrated, annually averaged steric anomaly in the Beaufort Gyre and Full Arctic based on satellite observations (bars), shown with the scaled Beaufort Gyre freshwater content anomaly from annual hydrographic surveys (purple line). (b, c) Inverse model solution contributions to the interannual steric changes for the (b) Full Arctic and (c) Beaufort Gyre budgets; each of the terms is presented as an anomaly from their mean value. (d) The net ocean transport into both budget regions in the inverse model solution. Two estimates of the observed net transports for the Full Arctic are also shown (Arctic Straits; Tsubouchi et al., 2019).

scaled freshwater content and steric anomalies than between the annual averages and August steric anomaly values (Figure S4 in Supporting Information S1). Our region is larger than that reported in Figure 11 of Proshutinsky et al. (2019), which is why our numbers are larger than the O(3500km^3) reported there.

Rabe et al. (2014) find an increase of about 7500km^3 from 2003 to 2012 in total Arctic freshwater content from in situ observations (relative to a reference salinity of 34), which agrees well with our scaled values (Figure 9a). However their updated time series through 2014 does not show the decline that we identify in 2013 and 2014 (Wang et al., 2019). Their analysis does not include Baffin Bay, the Barents or Kara Seas, and the Arctic Shelves, so this could be a source of disagreement. It could also be an issue with our satellite-based estimate after 2014 when our data sources change (see Section 3).

Solomon et al. (2021) present a satellite-based record of freshwater content following Giles et al. (2012) and Armitage et al. (2016). Although the freshwater content increase of about 7500km^3 from 2003 to 2008 in the Beaufort Gyre and Arctic agree well with our findings, they see a dramatic freshwater content decrease of 6000km^3 across the Arctic from 2008 to 2013. Solomon et al. (2021) do not include Baffin Bay or the Barents Sea in their calculation, but given the fact that our analysis agrees relatively well with Rabe et al. (2014), this significant disagreement is more likely to be due to the fact that they use a different satellite altimeter product than we do (Rose et al., 2019).

6.2. Ocean Fluxes

Our ocean flux term for the Full Arctic budget is based on the product presented in Tsubouchi et al. (2023), which is derived from all available simultaneous Arctic Strait data. However, our approach is fundamentally different than that of Tsubouchi et al. (2023). Their aim is to grid ocean observations in a physically consistent way and provide a detailed analysis of the associated ocean fluxes and transformations. Their zero salinity freshwater source term is initialized using its mean value and allowed to vary to satisfy the model constraints. They do not treat freshwater storage explicitly, but think of it as a part of their freshwater source term.

We are solving a different problem. Rather than treating freshwater storage as a residual term, we are seeking to find the likeliest explanation for known freshwater content changes given the observations of all freshwater source terms and their associated uncertainty. We argue that the net ocean flux is the least well-characterized term in the budget as it is a small difference between large inflows and outflows. The sea ice flux is better constrained, for example, as it is dominated by the export through Fram Strait and sea ice volume transports are smaller than ocean transports.

The changes made to the annual mean ocean volume transports by the inverse model in order to explain the observed freshwater content changes are on the order of 50 mSv, which is much smaller than we can reliably measure on these scales. That the measurements could be off by this much (in a random fashion) seems entirely plausible (Figure 9). We have not, however, quantified how much the density would have to change and where. It is not likely to be a dramatic change as the mass equivalent and volume transports follow each other closely in the inverse model solution as they do in the initial estimate (Figures S10 and S11 in Supporting Information S1).

Interestingly, the seasonal cycle of the Full Arctic ocean flux inverse model solution is inverted and has about twice the amplitude of the observation-based initial condition (from ≈200 mSv to ≈400 mSv, Figure S10 in Supporting Information S1). This adjustment seems somewhat less plausible than the adjustment of the annual mean fluxes (are the ocean measurements of the seasonality really out of phase with reality?) and is likely an artifact of either our or Tsubouchi et al.'s framework. For example, the satellite measurements may underestimate the seasonality of the steric height.

It would be illuminating to combine our approach with that of Tsubouchi et al. (2023). And identify more specifically how ocean fields would have to change to explain the observed freshwater content changes, particularly in the under-observed shelf portions of the freshwater outflow east of Greenland. Additional dynamical insight could be obtained by calculating mass, volume, steric, and freshwater budgets in the Arctic Subpolar gyre sTate Estimate (ASTE R1, Nguyen et al., 2021), which is an ocean-sea ice model-data synthesis over 2002–2017. Mean ocean transports at major Arctic straits in ASTE R1 are in agreement within uncertainty with the independent estimates of Tsubouchi et al. (see Figure 15 of Nguyen et al., 2021).

6.3. Sea Ice Melt

Sea ice melt is not a positive freshwater source in our liquid freshwater budget for the Full Arctic. In fact, there is more sea ice growth in our Full Arctic region than melt, so sea ice melt is a negative term in our integrated steric budget (Figure 5c). We also do not find that sea ice melt contributes significantly to interannual variability in Arctic freshwater content (Figure 9b), except perhaps to the freshwater content decline of 2013 and 2014. This result stands in contrast to the findings of Haine et al. (2015), who cite sea ice melt as an important source of freshwater to the Arctic based on the observed sea ice decline, but is in agreement with the findings of Wang et al. (2019), who argue that increasing Arctic freshwater content is not a result of sea ice decline.

Our Beaufort Gyre freshwater budget also shows net sea ice growth and export from the region. This differs from the results of Proshutinsky et al. (2019) and Krishfield et al. (2014), who find net sea ice convergence in the Beaufort Gyre region. Their findings are based on Polar Pathfinder sea ice motion vectors and sea ice thickness from upward looking sonar as well as sea ice thickness inferred from satellite microwave brightness temperature data (Tateyama et al., 2002; Tschudi et al., 2020), whereas our findings are based on PIOMAS. We compare monthly sea ice thickness estimates from PIOMAS and the Beaufort Gyre Observing System upward looking sonar (Figure S9 in Supporting Information S1) and find generally good correspondence, but PIOMAS does appear to overestimate thickness at the seasonal sea ice maxima, which has also been reported by Schweiger et al. (2011) and Solomon et al. (2021). Our results agree with Proshutinsky et al. (2019), in that the sea ice melt term is much smaller than freshwater from rivers.

6.4. Framework-Related Uncertainties

In this study, we seek to explain the observed Arctic steric changes by varying the source terms in proportion to their uncertainty in an inverse model framework. We hence assign the satellite measurements of volume and mass storage zero uncertainty, which we know is not the case. The satellite measurements have been validated by other studies (Armitage et al., 2016; Peralta-Ferriz et al., 2014) and we find that seasonal variability measured by GRACE agrees well with moored bottom pressure sensors on the Beaufort Gyre Observing System moorings (Figure S13 in Supporting Information S1). Furthermore, the reasonable agreement between our scaled freshwater content and the satellite changes in the Beaufort Gyre is encouraging (Figures 2c and 9a). Hence, the satellites are known to reproduce the interannual patterns of freshwater change on the large scale and we seek to connect these to the changes in the sources. At the same time, the GRACE satellite has very coarse resolution, and both satellites have measurement uncertainty, particularly near the coast. Factoring this uncertainty in and continuing to ground-truth satellites with in situ measurements are important avenues for future work.

Connecting the Arctic Ocean's steric budget to its freshwater budget relies on the fact that the Arctic's density is controlled by salinity. We validated this claim (Figures S1–S3 in Supporting Information S1) and found that this holds within the Arctic, but is not necessarily the case in the Arctic Straits. A more detailed examination of how ocean fluxes are connected to steric changes (as suggested in Section 6.2), will also need to take temperature into account. As the Arctic Ocean "spices up" (Timmermans & Jayne, 2016), the assumption that steric changes correspond to freshwater changes will no longer hold. Along the same lines, we neglect surface heating in our volume budget, which is justified given that surface cooling and heating is buffered by sea ice growth and melt, and the seasonal cycle of Arctic Ocean density change is dominated by salinity changes (Figure S1a in Supporting Information S1). However, as the Arctic Ocean becomes seasonally ice free, this will no longer hold and surface heating will need to be factored in.

7. Conclusions

In this study, we introduce an Arctic Ocean freshwater budget framework based on volume and mass budgets. We explain and justify the connection between Arctic steric changes and freshwater changes and capitalize on the fact that Arctic Ocean mass and volume have been measured by satellite since 2003. The steric changes measured by satellite compare well with in situ observations of freshwater content changes (Morison et al., 2012; Proshutinsky et al., 2019; Rabe et al., 2014) and we seek to connect these changes to changes in freshwater source terms: river runoff, precipitation minus evaporation, land ice melt, sea ice export, sea ice melt, and ocean fluxes. Using an

inverse model that is constrained using observation-based uncertainty, we find that changing ocean fluxes are the most likely driver of decadal freshwater content changes in the Arctic Ocean.

This conclusion is not based on observed changes to the ocean fluxes, but comes about because the ocean flux has the largest uncertainty of any of the freshwater source terms. This is an inherent feature of the ocean flux term because it is the difference between large flows O(10 Sv), whereas the next largest freshwater sources are O (100 mSv). We also do not find significant changes in the other freshwater source terms from 2003 to 2020, as was also noted for the meteoric components (rivers, net precipitation, and glacial meltwater) from 2003 to 2008 by Alkire et al. (2017). The changes that would be required of the observed net ocean fluxes to explain the inter-decadal freshwater content changes are O(10 mSv) and are hence entirely plausible (Figure 9, see Section 6.2 for a detailed discussion).

We find little freshwater compensation between the Beaufort Gyre and the rest of the Arctic Ocean. Instead, we find that Arctic freshwater content changes are dominated by changes in the Beaufort Gyre and that changes in the two regions are relatively synchronous (Figures 2 and 9, see Section 6.1 for more context). In other words, the freshwater that accumulates in the Beaufort Gyre originates from beyond our Full Arctic domain. If freshwater content changes are indeed controlled by ocean fluxes in and out of these domains, the implication is that there is a large-scale coupling between fluxes into the Arctic through the Straits and into the Beaufort Gyre. For example, when the Beaufort High is stronger, linked atmospheric patterns tend to draw in more freshwater through the Bering Strait, or release less into the Atlantic. This idea requires deeper physical understanding and could be investigated further by analyzing atmospheric fields and/or using ocean models, but one of its potential implications is that freshwater released from the Beaufort Gyre is exported to the Atlantic relatively quickly (within a year), where it could influence globally important water mass transformation processes.

Our volume, mass, and steric budgets for the Arctic Ocean and Beaufort Gyre regions provide physically consistent and reference-salinity-free benchmarks for comparison to model output. Because they are independent of reference salinity, comparisons will not necessarily be limited by known model salinity biases and could instead enable diagnosis of the processes driving different aspects of the budgets, which we do not do in this study. The framework presented in this study could also provide the basis for continuing to monitor the Arctic's freshwater budget. One potential concern is that it requires more accurate measurements of the net ocean fluxes through the Arctic Straits. However, this source of uncertainty exists at the foundation of all nonstationary freshwater budgets, so that using a framework that highlights it can be seen as an advantage.

Data Availability Statement

All Arctic dynamic topography/geostrophic currents data were provided by the Centre for Polar Observation and Modelling, University College London (Armitage et al., 2016, 2017). They were downloaded on 4 August 2023 from http://www.cpom.ucl.ac.uk/dynamic_topography. JPL GRACE and GRACE-FO Mascon Ocean, Ice, and Hydrology Equivalent Water Height CRI Filtered Release 06.1 Version 03 (Watkins et al., 2015; Wiese et al., 2016) were downloaded on 4 August 2023 from https://podaac.jpl.nasa.gov/dataset/TELLUS_GRAC-GRFO_MASCON_CRI_GRID_RL06.1_V3. River discharge data were accessed on 14 July 2023 from https://arcticgreatrivers.org/discharge/ (McClelland et al., 2023). ERA5 data were accessed on 10 July 2023 from the Copernicus Climate Change Service (C3S) Climate Data Store: https://cds.climate.copernicus.eu/datasets/reanalysis-era5-single-levels-monthly-means (Copernicus Climate Change Service, 2017). Land ice data were downloaded from the British Oceanographic Data Centre on 14 July 2023 from the British Oceanographic Data Centre at https://doi.org/10.5285/77dff70c-2ae7-2e66-e053-6c86abc05dc6 (Bamber et al., 2018a, 2018b). Arctic Strait inverse model solutions for ocean and sea ice properties and transport are available from https://doi.org/10.1594/PANGAEA.909966 (Tsubouchi et al., 2019). World Ocean Atlas 2023 data were downloaded on 13 October 2023 from https://www.ncei.noaa.gov/access/world-ocean-atlas-2023/ (Locarnini et al., 2023; Reagan et al., 2023). The Beaufort Gyre Observing System hydrographic survey data and freshwater content data products are available at https://www2.whoi.edu/site/beaufortgyre/data/ and the NSF's Arctic data center (https://arcticdata.io/catalog/portals/beaufortgyre). The Pan-Arctic Ice-Ocean Modeling and Assimilation System (PIOMAS) model grid data (Zhang & Rothrock, 2003) were downloaded on 14 July 2023 from http://psc.apl.uw.edu/research/projects/arctic-sea-ice-volume-anomaly/data/model_grid using https://github.com/Weiming-Hu/PyPIOMAS/.

Acknowledgments
We thank two reviewers, whose meticulous and constructive feedback greatly improved this manuscript. This work was supported by the US National Science Foundation Office of Polar Programs Arctic Observing Network grants #1949881 and #1950077. We are grateful to Andrey Proshutinsky, Rick Krishfield, and the many scientists, technicians, and mariners who have supported the Beaufort Gyre Observing System program.

References

Aagaard, K., & Carmack, E. C. (1989). The role of sea ice and other fresh water in the Arctic circulation. *Journal of Geophysical Research*, *94*(C10), 14485–14498. https://doi.org/10.1029/JC094iC10p14485

Alkire, M. B., Morison, J., Schweiger, A., Zhang, J., Steele, M., Peralta-Ferriz, C., & Dickinson, S. (2017). A meteoric water budget for the Arctic Ocean. *Journal of Geophysical Research: Oceans*, *122*(12), 10020–10041. https://doi.org/10.1002/2017JC012807

Armitage, T. W., Bacon, S., Ridout, A. L., Petty, A. A., Wolbach, S., & Tsamados, M. (2017). Arctic Ocean surface geostrophic circulation 2003-2014. *The Cryosphere*, *11*(4), 1767–1780. https://doi.org/10.5194/tc-11-1767-2017

Armitage, T. W., Bacon, S., Ridout, A. L., Thomas, S. F., Aksenov, Y., & Wingham, D. J. (2016). Arctic sea surface height variability and change from satellite radar altimetry and GRACE, 2003-2014. *Journal of Geophysical Research: Oceans*, *121*(9), 4303–4322. https://doi.org/10.1002/2015JC011579

Babb, D. G., Galley, R. J., Howell, S. E. L., Landy, J. C., Stroeve, J. C., & Barber, D. G. (2022). Increasing multiyear sea ice loss in the Beaufort Sea: A new export pathway for the diminishing multiyear ice cover of the Arctic Ocean. *Geophysical Research Letters*, *49*(9), e2021GL097595. https://doi.org/10.1029/2021GL097595

Bacon, S., Aksenov, Y., Fawcett, S., & Madec, G. (2015). Arctic mass, freshwater and heat fluxes: Methods and modelled seasonal variability. *Philosophical Transactions of the Royal Society A: Mathematical, Physical & Engineering Sciences*, *373*(2052), 20140169. https://doi.org/10.1098/rsta.2014.0169

Bacon, S., Garabato, A. C. N., Aksenov, Y., Brown, N. J., & Tsubouchi, T. (2022). Arctic Ocean boundary exchanges: A review. *Oceanography*, *35*(3/4), 94–102.

Bamber, J. L., Tedstone, A. J., King, M. D., Howat, I. M., Enderlin, E., Van Den Broeke, M., & Noel, B. P. Y. (2018a). Modelled and observational freshwater flux time series for land ice in the Arctic and North Atlantic for 1958-2016 b. https://doi.org/10.5285/77dff70c-2ae7-2e66-e053-6c86abc05dc6

Bamber, J. L., Tedstone, A. J., King, M. D., Howat, I. M., Enderlin, E. M., van den Broeke, M. R., & Noel, B. (2018b). Land ice freshwater budget of the Arctic and north Atlantic oceans: 1. Data, methods, and results. *Journal of Geophysical Research: Oceans*, *123*(3), 1827–1837. https://doi.org/10.1002/2017JC013605

Barrett, A. P., Stroeve, J. C., & Serreze, M. C. (2020). Arctic Ocean precipitation from atmospheric reanalyses and comparisons with north pole drifting station records. *Journal of Geophysical Research: Oceans*, *125*(1), e2019JC015415. https://doi.org/10.1029/2019JC015415

Bintanja, R., van der Wiel, K., van der Linden, E. C., Reusen, J., Bogerd, L., Krikken, F., & Selten, F. M. (2020). Strong future increases in Arctic precipitation variability linked to poleward moisture transport. *Science Advances*, *6*(7), eaax6869. https://doi.org/10.1126/sciadv.aax6869

Boisvert, L. N., Webster, M. A., Petty, A. A., Markus, T., Bromwich, D. H., & Cullather, R. I. (2018). Intercomparison of precipitation estimates over the Arctic Ocean and its peripheral seas from reanalyses. *Journal of Climate*, *31*(20), 8441–8462. https://doi.org/10.1175/JCLI-D-18-0125.1

Carmack, E. C. (2007). The alpha/beta ocean distinction: A perspective on freshwater fluxes, convection, nutrients and productivity in high-latitude seas. *Deep-Sea Research Part II Topical Studies in Oceanography*, *54*(23–26), 2578–2598. https://doi.org/10.1016/j.dsr2.2007.08.018

Carmack, E. C., Yamamoto-Kawai, M., Haine, T. W. N., Bacon, S., Bluhm, B. A., Lique, C., et al. (2016). Freshwater and its role in the Arctic Marine System: Sources, disposition, storage, export, and physical and biogeochemical consequences in the Arctic and global oceans. *Journal of Geophysical Research: Biogeosciences*, *121*(3), 675–717. https://doi.org/10.1002/2015JG003140

Chambers, D. P., & Bonin, J. A. (2012). Evaluation of Release-05 GRACE time-variable gravity coefficients over the ocean. *Ocean Science*, *8*(5), 859–868. https://doi.org/10.5194/os-8-859-2012

Copernicus Climate Change Service. (2017). *ERA5: Fifth generation of ECMWF atmospheric reanalyses of the global climate*. Copernicus Climate Change Service Climate Data Store (CDS). https://doi.org/10.24381/cds.f17050d7

Dee, D. P., Uppala, S. M., Simmons, A. J., Berrisford, P., Poli, P., Kobayashi, S., et al. (2011). The ERA-Interim reanalysis: Configuration and performance of the data assimilation system. *Quarterly Journal of the Royal Meteorological Society*, *137*(656), 553–597. https://doi.org/10.1002/qj.828

Fukumori, I., Wang, O., & Fenty, I. (2021). Causal mechanisms of sea level and freshwater content change in the Beaufort Sea. *Journal of Physical Oceanography*, *51*(10), 3217–3234. https://doi.org/10.1175/JPO-D-21-0069.1

Giles, K. A., Laxon, S. W., Ridout, A. L., Wingham, D. J., & Bacon, S. (2012). Western Arctic Ocean freshwater storage increased by wind-driven spin-up of the Beaufort Gyre. *Nature Geoscience*, *5*(3), 194–197. https://doi.org/10.1038/ngeo1379

Haine, T. W. N., Curry, B., Gerdes, R., Hansen, E., Karcher, M., Lee, C., et al. (2015). Arctic freshwater export: Status, mechanisms, and prospects. *Global and Planetary Change*, *125*, 13–35. https://doi.org/10.1016/J.GLOPLACHA.2014.11.013

Haine, T. W. N., Siddiqui, A. H., & Jiang, W. (2023). Arctic freshwater impact on the Atlantic Meridional Overturning Circulation: Status and prospects. *Philosophical Transactions of the Royal Society A: Mathematical, Physical & Engineering Sciences*, *381*(2262), 20220185. https://doi.org/10.1098/rsta.2022.0185

Howell, S. E. L., Brady, M., Derksen, C., & Kelly, R. E. J. (2016). Recent changes in sea ice area flux through the Beaufort Sea during the summer. *Journal of Geophysical Research: Oceans*, *121*(4), 2659–2672. https://doi.org/10.1002/2015JC011464

Jenkins, A., & Holland, D. (2007). Melting of floating ice and sea level rise. *Geophysical Research Letters*, *34*(16). https://doi.org/10.1029/2007GL030784

Krishfield, R. A., Proshutinsky, A., Tateyama, K., Williams, W. J., Carmack, E. C., McLaughlin, F. A., & Timmermans, M. L. (2014). Deterioration of perennial sea ice in the Beaufort Gyre from 2003 to 2012 and its impact on the oceanic freshwater cycle. *Journal of Geophysical Research: Oceans*, *119*(2), 1271–1305. https://doi.org/10.1002/2013JC008999

Kwok, R., Cunningham, G. F., Wensnahan, M., Rigor, I., Zwally, H. J., & Yi, D. (2009). Thinning and volume loss of the Arctic Ocean sea ice cover: 2003–2008. *Journal of Geophysical Research*, *114*(C7). https://doi.org/10.1029/2009JC005312

Laxon, S. W., Giles, K. A., Ridout, A. L., Wingham, D. J., Willatt, R., Cullen, R., et al. (2013). CryoSat-2 estimates of Arctic sea ice thickness and volume. *Geophysical Research Letters*, *40*(4), 732–737. https://doi.org/10.1002/grl.50193

Le Bras, I. A.-A., Straneo, F., Muilwijk, M., Smedsrud, L. H., Li, F., Lozier, M. S., & Holliday, N. P. (2021). How much Arctic fresh water participates in the subpolar overturning circulation? *Journal of Physical Oceanography*, *51*(3), 955–973. https://doi.org/10.1175/JPO-D-20-0240.1

Lin, P., Pickart, R. S., Heorton, H., Tsamados, M., Itoh, M., & Kikuchi, T. (2023). Recent state transition of the Arctic Ocean's Beaufort Gyre. *Nature Geoscience*, *16*(6), 485–491. https://doi.org/10.1038/s41561-023-01184-5

Lindsay, R. W., & Zhang, J. (2006). Assimilation of ice concentration in an ice–ocean model. *Journal of Atmospheric and Oceanic Technology*, *23*(5), 742–749. https://doi.org/10.1175/JTECH1871.1

Locarnini, R. A., Baranova, O. K., Mishonov, A. V., Boyer, T. P., Reagan, J. R., Dukhovskoy, D., et al. (2023). World Ocean Atlas 2023. In A. Mishonov (Technical Ed.), *Temperature* (Vol. 1). NOAA Atlas NESDIS.

McClelland, J., Tank, S., Spencer, R., Shiklomanov, A., Zolkos, S., & Holmes, R. (2023). Arctic Great Rivers Observatory. Discharge Dataset, Version 20230227. https://arcticgreatrivers.org/data/

McPhee, M. G., Proshutinsky, A., Morison, J. H., Steele, M., & Alkire, M. B. (2009). Rapid change in freshwater content of the Arctic Ocean. *Geophysical Research Letters*, *36*(10), 1–6. https://doi.org/10.1029/2009GL037525

Meier, W. N., & Stroeve, J. (2022). An updated assessment of the changing Arctic Sea ice cover. *Oceanography*, *35*(3/4), 10–19. https://doi.org/10.5670/oceanog.2022.114

Moore, G. W. K., Schweiger, A., Zhang, J., & Steele, M. (2019). Spatiotemporal variability of sea ice in the Arctic's last ice area. *Geophysical Research Letters*, *46*(20), 11237–11243. https://doi.org/10.1029/2019GL083722

Morison, J., Kwok, R., Peralta-Ferriz, C., Alkire, M., Rigor, I., Andersen, R., & Steele, M. (2012). Changing Arctic Ocean freshwater pathways. *Nature*, *481*(7379), 66–70. https://doi.org/10.1038/nature10705

Nguyen, A. T., Pillar, H., Ocaña, V., Bigdeli, A., Smith, T. A., & Heimbach, P. (2021). The Arctic Subpolar Gyre sTate Estimate: Description and assessment of a data-constrained, dynamically consistent ocean-sea ice estimate for 2002–2017. *Journal of Advances in Modeling Earth Systems*, *13*(5), e2020MS002398. https://doi.org/10.1029/2020MS002398

Noerdlinger, P. D., & Brower, K. R. (2007). The melting of floating ice raises the ocean level. *Geophysical Journal International*, *170*(1), 145–150. https://doi.org/10.1111/j.1365-246X.2007.03472.x

Peralta-Ferriz, C., & Morison, J. (2010). Understanding the annual cycle of the Arctic Ocean bottom pressure. *Geophysical Research Letters*, *37*(10). https://doi.org/10.1029/2010GL042827

Peralta-Ferriz, C., Morison, J. H., Wallace, J. M., Bonin, J. A., & Zhang, J. (2014). Arctic Ocean circulation patterns revealed by GRACE. *Journal of Climate*, *27*(4), 1445–1468. https://doi.org/10.1175/JCLI-D-13-00013.1

Perovich, D. K., Grenfell, T. C., Light, B., Elder, B. C., Harbeck, J., Polashenski, C., et al. (2009). Transpolar observations of the morphological properties of Arctic sea ice. *Journal of Geophysical Research*, *114*(C1). https://doi.org/10.1029/2008JC004892

Proshutinsky, A., Krishfield, R., Timmermans, M.-L., Toole, J., Carmack, E., McLaughlin, F., et al. (2009). Beaufort Gyre freshwater reservoir: State and variability from observations. *Journal of Geophysical Research*, *114*(C1), C00A10. https://doi.org/10.1029/2008JC005104

Proshutinsky, A., Krishfield, R., Toole, J. M., Timmermans, M. L., Williams, W., Zimmermann, S., et al. (2019). Analysis of the Beaufort Gyre freshwater content in 2003-2018. *Journal of Geophysical Research: Oceans*, *124*(12), 1–32. https://doi.org/10.1029/2019JC015281

Rabe, B., Karcher, M., Kauker, F., Schauer, U., Toole, J. M., Krishfield, R. A., et al. (2014). Arctic Ocean basin liquid freshwater storage trend 1992 – 2012. *Geophysical Research Letters*, *41*(3), 961–968. https://doi.org/10.1002/2013GL058121.ice

Reagan, J. R., Dukhovskoy, D., Seidov, D., Boyer, T. P., Locarnini, R. A., Baranova, O. K., et al. (2023). World Ocean Atlas 2023. In : A. Mishonov (Technical Ed.), *Salinity* (Vol. 2). NOAA Atlas NESDIS.

Ricker, R., Girard-Ardhuin, F., Krumpen, T., & Lique, C. (2018). Satellite-derived sea ice export and its impact on Arctic ice mass balance. *The Cryosphere*, *12*(9), 3017–3032. https://doi.org/10.5194/tc-12-3017-2018

Rose, S. K., Andersen, O. B., Passaro, M., Ludwigsen, C. A., & Schwatke, C. (2019). Arctic Ocean sea level record from the complete radar altimetry era: 1991–2018. *Remote Sensing*, *11*(14), 1672. https://doi.org/10.3390/rs11141672

Schauer, U., & Losch, M. (2019). Freshwater in the ocean is not a useful parameter in climate research. *Journal of Physical Oceanography*, *49*(9), 2309–2321. JPO-D-19-0102.1. https://doi.org/10.1175/JPO-D-19-0102.1

Schweiger, A., Lindsay, R., Zhang, J., Steele, M., Stern, H., & Kwok, R. (2011). Uncertainty in modeled Arctic sea ice volume. *Journal of Geophysical Research*, *116*(C8), C00D06. https://doi.org/10.1029/2011JC007084

Serreze, M. C., Barrett, A. P., Slater, A. G., Woodgate, R. A., Aagaard, K., Lammers, R. B., et al. (2006). The large-scale freshwater cycle of the Arctic. *Journal of Geophysical Research*, *111*(C11). https://doi.org/10.1029/2005JC003424

Solomon, A., Heuzé, C., Rabe, B., Bacon, S., Bertino, L., Heimbach, P., et al. (2021). Freshwater in the Arctic Ocean 2010–2019. *Ocean Science*, *17*(4), 1081–1102. https://doi.org/10.5194/os-17-1081-2021

Stadnyk, T. A., Tefs, A., Broesky, M., Déry, S. J., Myers, P. G., Ridenour, N. A., et al. (2021). Changing freshwater contributions to the Arctic: A 90-year trend analysis (1981–2070). *Elementa: Science of the Anthropocene*, *9*(1), 00098. https://doi.org/10.1525/elementa.2020.00098

Steele, M., Zhang, J., & Ermold, W. (2010). Mechanisms of summertime upper Arctic Ocean warming and the effect on sea ice melt. *Journal of Geophysical Research*, *115*(C11). https://doi.org/10.1029/2009JC005849

Sumata, H., de Steur, L., Gerland, S., Divine, D. V., & Pavlova, O. (2022). Unprecedented decline of Arctic sea ice outflow in 2018. *Nature Communications*, *13*(1), 1747. https://doi.org/10.1038/s41467-022-29470-7

Suzuki, T., Yamazaki, D., Tsujino, H., Komuro, Y., Nakano, H., & Urakawa, S. (2018). A dataset of continental river discharge based on JRA-55 for use in a global ocean circulation model. *Journal of Oceanography*, *74*(4), 421–429. https://doi.org/10.1007/s10872-017-0458-5

Tateyama, K., Enomoto, H., Toyota, T., & Uto, S. (2002). Sea ice thickness estimated from passive microwave radiometers. *Polar Meteorology and Glaciology*, *16*, 15–31. https://doi.org/10.15094/00002943

Timmermans, M.-L., & Jayne, S. R. (2016). The Arctic Ocean spices up. *Journal of Physical Oceanography*, *4*, 1277–1284. https://doi.org/10.1175/JPO-D-16-0027.1

Timmermans, M.-L., & Toole, J. M. (2023). The Arctic Ocean's Beaufort Gyre. *Annual Review of Marine Science*, *15*(1), 223–248. https://doi.org/10.1146/annurev-marine-032122-012034

Tschudi, M. A., Meier, W. N., & Stewart, J. S. (2020). An enhancement to sea ice motion and age products at the National Snow and Ice Data Center (NSIDC). *The Cryosphere*, *14*(5), 1519–1536. https://doi.org/10.5194/tc-14-1519-2020

Tsubouchi, T., Bacon, S., Aksenov, Y., Garabato, A. C. N., Beszczynska-Möller, A., Hansen, E., et al. (2018). The Arctic Ocean seasonal cycles of heat and freshwater fluxes: Observation-based inverse estimates. *Journal of Physical Oceanography*, *48*(9), 2029–2055. https://doi.org/10.1175/JPO-D-17-0239.1

Tsubouchi, T., Bacon, S., Naveira Garabato, A. C., Aksenov, Y., Laxon, S. W., Fahrbach, E., et al. (2012). The Arctic Ocean in summer: A quasi-synoptic inverse estimate of boundary fluxes and water mass transformation. *Journal of Geophysical Research*, *117*(1), 1–28. https://doi.org/10.1029/2011JC007174

Tsubouchi, T., von Appen, W.-J., Kanzow, T., & de Steur, L. (2023). Temporal variability of the overturning circulation in the Arctic Ocean and the associated heat and freshwater transports during 2004-2010. *Journal of Physical Oceanography*, *1*(aop). https://doi.org/10.1175/JPO-D-23-0056.1

Tsubouchi, T., von Appen, W.-J., Schauer, U., Kanzow, T., Lee, C., Curry, B., et al. (2019). *The Arctic Ocean volume, heat and fresh water transports time series from October 2004 to May 2010*. PANGAEA. https://doi.org/10.1594/PANGAEA.909966

Tsujino, H., Urakawa, S., Nakano, H., Small, R. J., Kim, W. M., Yeager, S. G., et al. (2018). JRA-55 based surface dataset for driving ocean–sea-ice models (JRA55-do). *Ocean Modelling*, *130*, 79–139. https://doi.org/10.1016/j.ocemod.2018.07.002

Wang, Q., Wekerle, C., Danilov, S., Sidorenko, D., Koldunov, N., Sein, D., et al. (2019). Recent sea ice decline did not significantly increase the total liquid freshwater content of the Arctic Ocean. *Journal of Climate*, *32*(1), 15–32. https://doi.org/10.1175/JCLI-D-18-0237.1

Watkins, M. M., Wiese, D. N., Yuan, D.-N., Boening, C., & Landerer, F. W. (2015). Improved methods for observing Earth's time variable mass distribution with GRACE using spherical cap mascons. *Journal of Geophysical Research: Solid Earth*, *120*(4), 2648–2671. https://doi.org/10.1002/2014JB011547

Wiese, D. N., Landerer, F. W., & Watkins, M. M. (2016). Quantifying and reducing leakage errors in the JPL RL05M GRACE Mascon solution. *Water Resources Research*, *52*(9), 7490–7502. https://doi.org/10.1002/2016WR019344

Winkelbauer, S., Mayer, M., Seitner, V., Zsoter, E., Zuo, H., & Haimberger, L. (2022). Diagnostic evaluation of river discharge into the Arctic Ocean and its impact on oceanic volume transports. *Hydrology and Earth System Sciences*, *26*(2), 279–304. https://doi.org/10.5194/hess-26-279-2022

Wunsch, C. (1996). *The ocean circulation inverse problem*. Cambridge University Press. https://doi.org/10.1017/CBO9780511629570

Zhang, J., & Rothrock, D. A. (2003). Modeling global sea ice with a thickness and enthalpy distribution model in generalized curvilinear coordinates. *Monthly Weather Review*, *131*(5), 845–861. https://doi.org/10.1175/1520-0493(2003)131⟨0845:MGSIWA⟩2.0.CO;2

Zhang, J., Weijer, W., Steele, M., Cheng, W., Verma, T., & Veneziani, M. (2021). Labrador Sea freshening linked to Beaufort Gyre freshwater release. *Nature Communications*, *12*(1), 1229. https://doi.org/10.1038/s41467-021-21470-3